BACKPULSE AND BACKBLOW CLEANING OF NANOFIBER FILTER LOADED WITH NANO-AEROSOLS

HAU WING YI CURIE

M.Phil

The Hong Kong Polytechnic University

2017

THE HONG KONG POLYTECHNIC UNIVERSITY

Department of Mechanical Engineering

Backpulse and Backblow Cleaning of Nanofiber Filter Loaded with Nano-aerosols

HAU Wing Yi Curie

A Thesis Submitted in Partial Fulfillment of the Requirements

for the Degree of Master of Philosophy

June 2016

CERTIFICATE OF ORIGINALITY

I hereby declare that this thesis is my own work and that, to the best of my knowledge and belief, it reproduces no material previously published or written, nor material that has been accepted for the award of any other degree or diploma, except where due acknowledgement has been made in the text.

(Signature)

HAU Wing Yi Curie (Name of student)

ABSTRACT

Electrospun nylon-6 nanofiber filter, with fiber diameters of 100 to 300nm, has been used for nano-aerosols filtration. Despite the effectiveness of filtration, the aerosol loading capacity of the filter is low and pressure drop across the filter increases rapidly with aerosol loading. This study examines the effectiveness of backpulse and backblow cleaning on nanofiber depth filter loaded with challenging polydispersed nano-aerosols with 50-60% less than 100 nm and maximum size less than 300-500nm. To investigate filter regeneration, a series of backpulses followed by backblow at constant air velocity was applied ona loaded nanofiber filter with maximum allowable pressure drop across the filter set at 600-1000Pa. The function of backpulse is to provide inertia to break-up the particle-particle locking as well as particle-fiber adhesion while backblow is to carry the loosened particles away from the filter.

Due to the fragility of nanofiber, a tri-nozzle setup has been introduced in the cleaning system to distribute the cleaning air relatively uniform across the filter instead of a concentrated jet targeted at the center of the filter that can damage nanofibers there. To optimize the cleaning conditions, the effect of several key parameters hasbeen investigated – pulse jet, flow durations, numbers of jet pulses, and applied pressure. Also, the filter properties, such as nanofiber diameteraffecting particle-fiber adhesion as well as particle capture, and

nanofiber filter thickness affecting particle capture and filter capacityhave been studied. Unfortunately, both have negative effects on filter cleaning by backpulse and backblow due to large adhesion force of particles to fibers for nanofiber filter with smaller fiber diameter and due to increasing recapture of loosened particles for a thick nanofiber filter, respectively.

For multilayer nanofiber filter, two inhomogeneous filters have been tested. One filter was made from a combo filter with a thickermicrofiber layer upstream and a thinner nanofiber layer downstream. The second filter was made from a nanofiber layer with mean fiber diameter of 280nm located upstream and another nanofiber layer with mean fiber diameter of 180nm located downstream. The cleaning effectiveness of the multilayer nanofiber filter was compared with a filter with only single nanofiber layer. The multi-layering configurationcan reduce the skin effect during aerosolloading, however, during cleaning with reversed flowthe downstream microfiber layer provided damping to the cleaning jet undermining the cleaning effectiveness on the upstream nanofiberlayer when compared to the case with regenerating only single nanofiber layer filter. For the filter with two nanofiberlayers, the downstream nanofiber layer enhanced the recapture of loosen particles during cleaning. Further, the presence of the downstream nanofiber layer also compromised the cleaning effectiveness of the nanofiber upstream layerduring reverse flow cleaning.

Cyclic filtration,involving both loading and cleaning, have been carried out in both single-layer and multilayer nanofiber filters. Both filter configurations have shown stable behavior in which the growth in residual pressure drop and the decrease in filtration cycle time were present primarily in the first filtration cycle (i.e. the conditioning phase) and subsequently both variables remained relatively constant thereafter. The pressure versus time during loading wasconvex upward for the first loading cycle (at times linear), but changed over to concave downward in subsequent cycles. This isdue to the dead pores of the filter being prefilledwith aerosols after the first loading and cleaning cycle.

PUBLICATIONS

Journals

Curie Wing-Yi Hau, Wallace Woon Fong Leung, “Experimental investigation of backpulse and backblow cleaning of nanofiber filter loaded with nano-aerosols”, Sep & Puri Tech J., 163, 30-38. doi: 10.1016/j.seppur.2016.02.041

Wallace Woon Fong Leung, Curie Wing-Yi Hau, “A model of backpulse and backblow cleaning of nanofiber filter loaded with nano-aerosols”,Sep & Puri Tech J., 169, 171-178. doi: 10.1016/j.seppur.2016.06.007

Conference

Hau W.Y.C., Leung W.W.F., (2014). Backpulse and backblow cleaning of nanofiber depth filter loaded with nanoaerosols. FPS 2014, European Conference on Fluid-Particle Separation, 15th- 17thOctober, 2014, Lyon, France.

ACKNOWLEDGEMENTS

First of all, I would like to express my sincere appreciation to my supervisor Prof. Wallace LEUNG for his guidance and support throughout thepast years. The research studycould not have been accomplished without his valuable advice and supervision. I also wish to show my gratitude to the Department of Mechanical Engineering of The Hong Kong Polytechnic University, for providing support with all the facilities for the research.I gratefully acknowledge the assistance of the following people from the Department of Mechanical Engineering of The Hong Kong Polytechnic University who shared their time and expertise to the completion of this research:Mr. Kwong-shing TSANG, Mr. Kwok-wai WONG, Mr. Ka-fung MAN, Mr. Wai-chiu WOO, Mr. Chi-wai MO, Mr. Benny LEUNG, and other staff.Specialthanksgotomy colleagues, Mr.Kent CHOY, Mr. Kenneth LO, Ms. Chun PEI and Ms. Eva MAK for their beneficial inspiration and encouragement throughout the project particularly during the difficult time.

I perceive these years as a big milestone and priceless lesson in my life. It is not only a gain in knowledge and skills but more about personalityand life lesson that will be useful in the future. I thank all the people who show their support directly and indirectly. Last but not least, my deepest sense of gratitude goesto my beloved family for their love and support as always.

TABLE OF CONTENTS

LIST OF FIGURES AND TABLES

LIST OF SYMBOLS AND ABBREVIATIONS

A	Filter frontal area[m^2]
E	Electric field strength[$\frac{\mathrm{V}}{\mathrm{m}}$]
N	Number of filtration cycles
U	Face velocity[$\frac{\mathrm{m}}{\mathrm{s}}$]
W	Mass deposition of dust on the filter[$\frac{\mathrm{g}}{\mathrm{m}^2}$]
Z	Fiber mat thickness[m]
c	Dust concentration[$\frac{\#}{\mathrm{cc}}$]
d	Standoff distance[m]
n	Number of jet pulses
μ	Dynamic viscosity[$\mathrm{Pa\ s}$]
η	Filtration efficiency
α_f	Packing density
D_p	Particle diameter[m]
d_f	Mean fiber diameter[m]
K_f^*	Specific resistance factor of the filter medium including the captured particles in the filter[m^{-1}]
K_c	Specific cake resistance[$\frac{\mathrm{m}}{\mathrm{kg}}$]
t_b	Backblow duration[s]
t_l	Loading time[hr]
ΔP	Pressure drop across filter[Pa]
ΔP_f	Pressure drop of cleanfilter[Pa]

ΔP_o	Pressure drop on loaded filter before cleaning[Pa]
ΔP_r	Pressure drop of filter after cleaning[Pa]
ΔP_c	Pressure drop across filter cake[Pa]
$\Delta P'$	Netpressure drop[Pa]
ΔP_f^*	Pressure drop across the nanofiber filter medium including the captured particles in the filter[Pa]
ΔV	Applied voltage[V]
MF	Mircofibrous Filter
NF	Nanofiber Filter
CMD	Count Median Diameter [nm]
GSD	Geometric Standard Deviation
HEPA	High efficiency particulate air
MMD	Mass Mean Diameter [nm]
MPPS	Most penetrating particle size
N6	Nylon 6
QF	Quality factor

Chapter 1

INTRODUCTION

1.1. Background and Literature Review

Nanoaerosols are air borne particles(air/liquid/solid)that are around 100 nm and smaller. They can be pollutants emitted from engines particularly in diesel engines or secondary pollutants formed that cause haze and smog, and viruses from common cold influenza viruses to epidemic viruses, such as middle-east respiratory syndrome virus (MERS) to bird flu virus (e.g.H5N1)(Hutten, I.M., 2007). Non-woven micro-fibrous filter, such asthe High Efficiency Particulate Air (HEPA) filter, can achieve up to 99.99% filtration efficiency but the pressure drop is extremely high reaching 300 to 1000Pa. Therefore, the alternativeof using nanofibers with fiber diameter of 90 to 300nm(J. Doshi, D.H. Reneker, 1995)has been investigated. Nanofiber filter can effectively capture nanoaerosols while maintaining relatively low pressure drop(J. Pich, 1966)(J.K.Lee, Y.Y.Ahn, S.K.Park, G.T.Kim, Y.H.Hwang, C.G.Lee, H.S.Shin, 2006), but microfiber filter is ineffective to capture these nanoaerosols despite that they can capture larger particles and can be reused by cleaning, especially for industrial applications.

Nanofibers are produced from electrospinning (Formhals, Producing of artificial fibers from fiber forming liquids, 1943)(Formhals, Artificial thread and method of producing same, 1940)(Formhals,

Method and apparatus for spinning, 1939)(Formhals, Process and apparatus for prearing artificial threads, 1934)(D. Li and Y. Xia, 2004)and the properties of nanofibers, such as fiber diameters, basis weight, etc. can be controlled by adjusting the conditions of electrospinning. Chowdhury and Stylios(M. Chowdhury, G. Stylios, 2010)have demonstratedthat the fiber diameter decreases with increasing applied electric field, where the electric field strength (E) is the ratio of applied voltage (ΔV) to standoff distance (d) (i.e. $E = \frac{\Delta V}{d}$).Other researchers (C. Huang, S. Chen, C. Lai, D. H. Reneker, H. Qiu, Y. Ye, H. Hou, 2006)(Z.M. Huanga, Y.Z. Zhang, M. Kotakic, S. Ramakrishna, 2003)suggested that polymer solution properties are also responsible for the electrospun fiber diameters and beads formation.*Figure 1.1* is the relationship between Nylon-4,6 solution concentration and average fiber diameter forneedle-typed electrospinning.

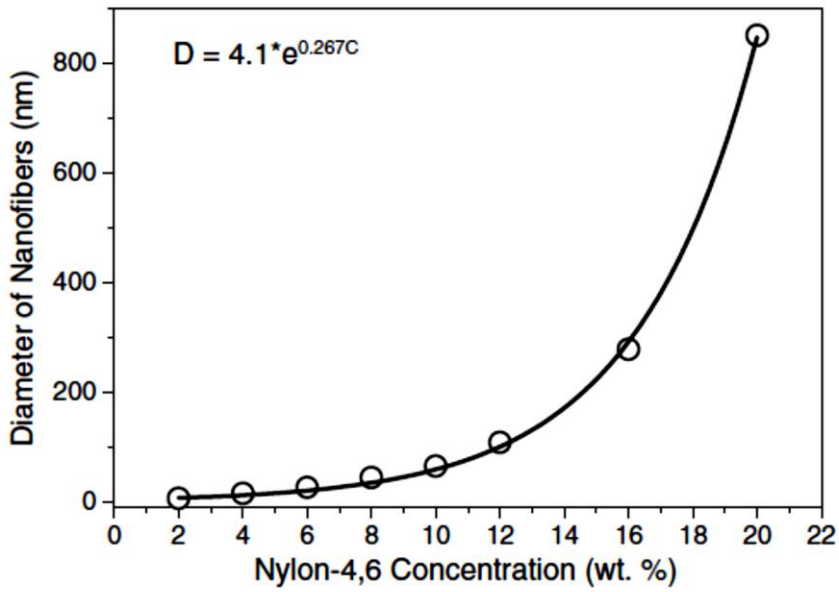

Figure 1.1Relationship of Nylon-4,6 solution concentration (wt. %) and fiber diameter in electrospinning(C. Huang, S. Chen, C. Lai, D. H. Reneker, H. Qiu, Y. Ye, H. Hou, 2006)

In aerosols separation, filters are typically divided into depth filter and surface filter, depends on its filtration mechanism. A surface filter captures particles directly on the upstream side, and the deposited particles then form bridges across the pores of the filter. Overtime, the accumulated particles form cake on the surface which becomes the effective filter media in the filtration process. For a depth filter, particles are trapped across the thickness of the filter by various force fields and mechanisms, namely inertial impaction, diffusion, interception and sieving.

For heavy particles, due to inertia, they are expected to continue with a straight path rather than follow the streamline, and get direct

impact on the fiber. This is inertial impaction where its effectiveness increases with face velocity of filtration. For light particles which have random walk instead of following the streamline are considered to be captured when they collide with or touches the fiber. Therefore, the effectiveness of diffusion increases when the face velocity decreases. Interception takes place for particles travel along the streamline are trapped when it touches the fiber while passing within one particle radius of the fibrous element. And sieving takes place when the particle diameter is larger than the gap between fibers. The particle will be collected and block the space.

However, the solid holding capacity for a thin nanofibers layer is very low (W .W.F. Leung, C.H. Hung, P.T. Yuen, 2010), thus a thicker nanofiber layer is more favourable serving as a depth filter with increasedservice life. Leung and Hung (W .W.F. Leung, C.H. Hung, 2012)found that the presence of “skin effect”in nanofiber depth filter for which the captured particleswere non-uniformly distributed across the filter thickness. More aerosolswere deposited in a layer at the upstream end of the filter whereas not much aerosols were deposited in the remaining filter downstream.

The aerosolsaccumulated at the thin skin region upstream of the filter contribute to the large and rapidincrease in pressure drop across the filter over time. At some point, the filtration changes from depth filtration to surface filtration for which a cake forms on the filter surface.

Over time, the pressure drop across the filter including the cake becomes so large thereby reducing the airflow through the filter to an unacceptable low level. At this point,the filter needs to be replaced. The filter can also be salvaged for reuse provided that it can be properly cleaned; however, it is unclear as to how the aerosols are redistributed after filter cleaning, in a favourable or unfavourable manner.

Numerous experimental studies on pulse-jet cleaning of baghouse and microfibrous filter have been carried out. Previous studies (M. De Ravin, W. Humphries, R. Postle, 1988)(J. Sievert, F. Löffler, 1989)(S. LAUX, U. RENZ, 1993)(R. Mai, M. Fronhöfer, H. Leibold, 1996) reported that the cleaning efficiency of microfiber filter is directly affected by the applied pressure. For backpulse cleaning of a baghouse filter, the cleaning effectiveness is dominated by the overpressure, which needs to be sufficiently high to overcome the adhesion force between the cake and the bagin order to detach particles from the bag. Humphries and Madden(W. Humphries, J.J. Madden, 1983)concluded that ineffective cleaning of pulse-bag filter is caused by using an applied pressure lower than the critical value, and moderate enhancement can be made in cleaning performance by increasing slightly the applied pressure over that of the critical value. Other parameters, such as standoff distance between nozzle and filter, jet duration, nozzle design, nozzle diameter, etc. were investigated as well (S. LAUX, U. RENZ, 1993)(H.C. Lu, C.J. Tsai, 1998)(H.C. Lu, C.J. Tsai, 1999)(H.C. Lu, C.J. Tsai, 1996)(S.K. Grannell, J.P.K. Seville, 1999)(J.H. Choi, Y.G. Seo, J.W. Chung,

2001)(L.M. Lo, D.R. Chen, D.Y.H. Pui, 2010). Granell and Seville(S.K. Grannell, J.P.K. Seville, 1999) conducted experiments to examine the influence of standoff distance between the nozzle and the inlet of a candle filter using backpulse cleaning. They found that too short standoff distance can lead to entrainment while long standoff distance can result in ineffective jet pulse. Laux(S. LAUX, U. RENZ, 1993) also found that the jet duration is a trivial factor on cleaning performance, as the overpressure which dominated cleaning did not increase with the jet duration. There are published guidelines for testing of cleanable filter media, such as VDI 3926 (Dr.-Ing. P. Gäng, 2002), but they are strictly written for cleaning of loaded baghouse and microfiber filters.

1.2. Project Objectives

The technology of backpulse cleaning of air filters is well-developed for baghouse and microfibrous filter. Whether the same knowhow can be applied to cleaning of a nanofiber filter is still anunknown as there has been virtually little in the literature on nanofiber filter cleaning. The fundamental issueis that whether nanoaerosols loaded nanofiber filter can be cleaned by using backpulse and backblow as the fiber diameter isonly of the order of 1/10 of microfiber filter and the fragility of the nanofibers during cleaning is a serious concern(the typical fiber diameter of microfiber filter is 2μm and for nanofiber filter is in hundreds nanometres).

Furthermore, we want to determine the filter condition after cleaning using backpulse and backblow. We are also interested to determine the filter cleaning effect due to (1) different jet configurations,for example, a concentrated air jet versus distributed air jets acting on the loaded nanofiber filter; (2) different jet settings, for example, the applied pressure and jet pulse durations; and (3) filter properties, such as, mean fiber diameter, and filter thickness.

Last but not least, we are interested in this project to determine the ultimate residual pressure drop levelafter backpulse and backblow, and the cyclic loading-and-cleaning behaviours of single and multilayer filters.

Chapter 2

METHODOLOGY

2.1. Fabrication of Nanofiber Filters by Electrospinning

Nylon (polyamide) was selected as the material for fabricating the test nanofiber filter due to its properties which are suitable for producing nanofibers by electrospinning. Nylon nanofibers have a smooth and simple fiber structure and Nylon is a chemically inert material well suited for different applications.

Nylon 6 (N6) pellet (6mm, Aldrich) was dissolved in formic acid to produce N6 solution. Subsequently, N6 nanofibers were fabricated by electrospinning the N6 solution under an applied electromagnetic field. The schematic of the needle-less electrospinning machine (NS Lab 200, Elmarco) is depicted in *Figure 2.1.* As seen, a highvoltage is applied to the needleless rotating electrode and the collecting electrode is grounded.

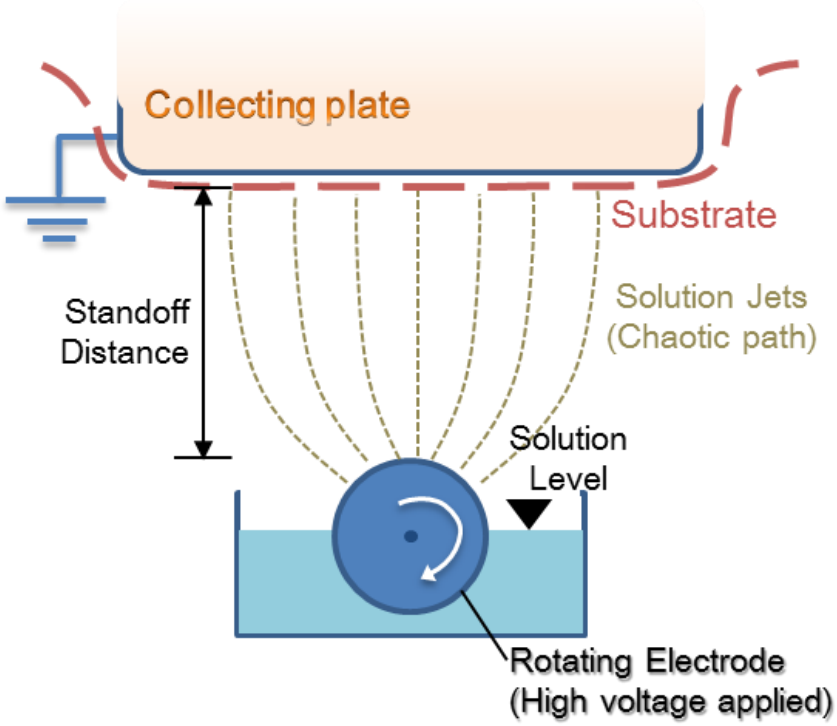

Figure 2.1The schematic of needle-less electrospinning machine (Elmarco, Cech Republic)

By adjusting the potential difference (40 – 80 kV), the standoff distance (10 – 19 cm) between the rotating electrode and the grounded collecting plate, the electrode rotating speed (6 – 50 Hz), and the concentration (14 – 22% by wt.) of the N6 precursor solution, nanofibers with mean fiber diameters ranging from 90 to 280 nm were produced in our laboratory. The fabrication of N6 nanofiber is favored under high electric field with sufficient time for solvent evaporation, it is highly depends on the specific laboratory environment and in our laboratory, the conditions are potential difference of 80kV and standoff distance of 15cm to 19 cm.The electrode rotating speed, depends on the viscosity of the precursor solution and the time for the taylor cone formation, says 20

Hz to 30 Hz. The solidosity (solid volume fraction) and the basis weight (mass of fiber per unit filter area) can be controlled by the electrospinning time in batch production, or by the travelling speed of the substrate material during continuous production, as well as the solution feeding rate by adjusting the electrode rotating speed during electrospinning.

The relationship between polymer solution concentration and the diameter of nanofibers depends primarily on the polymer used. Experiments were carried out in our laboratory to obtain the relationship between N6 solution concentration and the mean fiber diameter of electrospun nanofiber as shown in *Figure 2.2*.*Figure 2.2*shows that to obtain fiber diameters of 200nm, the solution concentration for N6 for electrospinning should be at 18% by wt. It is worthy to note that this result also depends on the specific electrospinning setup and conditions, such as operation temperature and relative humidity. The conditions for electrospinning are most favorable for producing nanofibers with fiber diameters of 100 to 300nm. It has beensuggested (J.K.Lee, Y.Y.Ahn, S.K.Park, G.T.Kim, Y.H.Hwang, C.G.Lee, H.S.Shin, 2006) that there is an active region for which a slight change in solution concentration would result in a large change in mean fiber diameter. *Figure 2.2* further confirms this result. Indeed, as the concentration increases from 18 to 20% by wt., the fiber diameter increases exponentially. Beyond this active region, increase in solution concentration only favors the formation of ribbon-shaped large fibers which are not desirable for

filtration application. On the other hand, at the other extreme it is more difficult to further decrease the mean fiber diameter by lowering the solution concentration beyond 12% by wt. An increase in applied voltage is also necessary to produce nanofibers with smaller diameter.

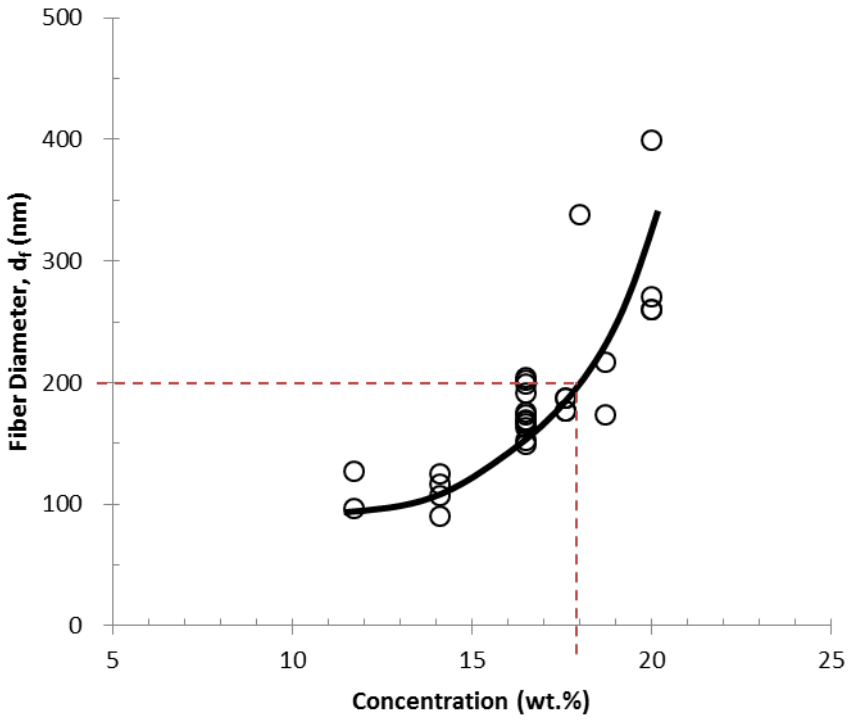

Figure 2.2The relationship of diameter of nanofibers with Nylon6 solution concentration obtained in our laboratory

The images of N6 nanofibers were obtained by Scanning Electron Microscope (SEM, JEOL Model JSM-6490, JEOL USA, Inc.) for determining mean fiber diameters as well as to ensure round cross-sectional fibers with uniform diameter, instead of obtaining other fibers shapes (such as ribbon-like) or beads, are obtained. Mean fiber diameter and fiber diameter distribution (*Figure2.4*) were estimated by

counting at least 100 fiber diameters obtained from the SEM images (*Figure 2.3*) by an image processing and analysis software, Image J (National Institutes of Health, US). The conditions of electrospun N6 nanofibers also depend on conductivity of the substrate material. Conventional substrate material in aerosol filtration is typically spunbond non-woven Polypropylene (PP) that has low conductivity, which hinders nanofibers production by electrospinning. Pre-treatment on the substrate is one of the several means to increase the conductivity to improve adhesion between the electrospun nanofibers and the substrate. The latter is very important as it allows effective backpulse and backblow on cleaning loaded nanofiber filter without nanofibers detaching from the substrate. By enhancing the wettability by use of a hydrophilic PP substrate,researchers have found that this improves the attachment of nanofibers ontothe substrate, which is highly desirable(F . Rombaldoni, K. Mahmood, A. Varesano, M.B. Songia, A. Aluhi, C. Vineis, G. Mazzuchetti, 2013)(W. Ren, C. Cheng, R. Wang, X. Li , 2010)(O.G. Armağan, B.K. Kayaoğlu, H.C. Karakaş, F.S. Güner, 2013).

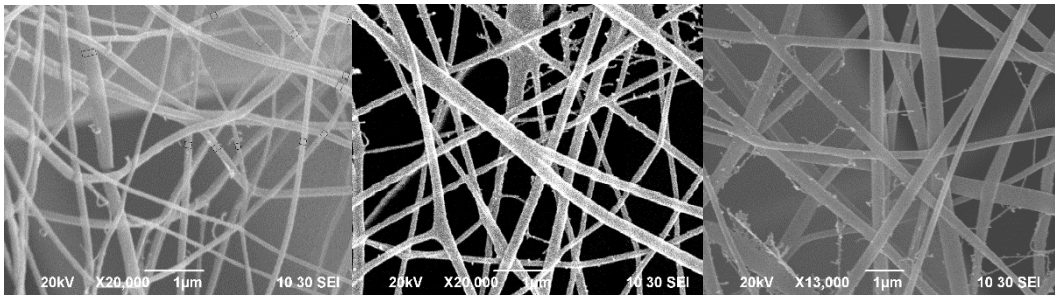

(a) (b) (c)

Figure 2.3Examples of SEM pictures of nanofibers with mean fiber diameter of (a)120nm, (b)180nm and (c)280nm

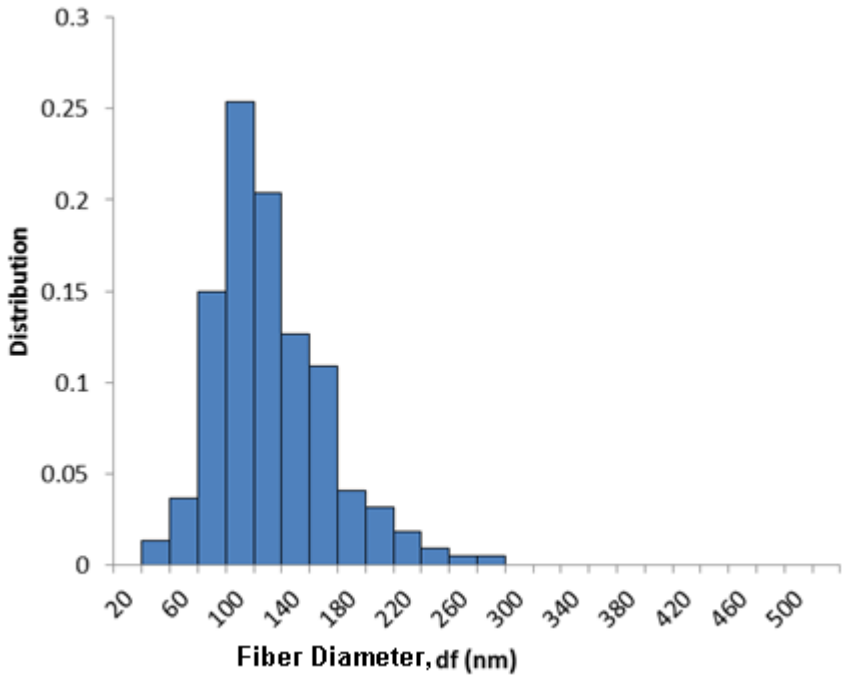

Figure 2.4Example of fiber diameter distribution counted from SEM pictures

2.2. Testing and Loading a Nanofiber Filter

The filter is loaded with aerosols over time until a cake forms on the surface of the filter. Once a cake is formed, the pressure drop across the loaded filter reflects the amount of cake on the filter surface with higher pressure drop indicative of a thicker cake, and vice versa. Thus, the end point on aerosol loading on a filter can be set by the maximum pressure drop across the filter. This point can be arbitrary and once it is set, the

time of operating the filter to reach this end point actually reduces progressively over time. Alternatively, one can prescribe the maximum operation duration and the filter is loaded with cake on the filter surface and the maximum pressure drop reached at the end point progressively increases. This is because after each cycle cleaning does not remove all the aerosols depositedon the filter resulting in residual aerosols left in the filter trapped in “dead spots”. These residual aerosols left in the filter become a trap for additional incoming aerosols in the subsequent loading andcleaning stage. Loading a test filter using ambient air suffers from uncontrolled aerosols size, distribution concentration, and composition, all of which may vary over time. It would be very difficult to draw comparison between different filter configurations as the feed aerosols are changing over the test period. To have a consistent aerosol loading on the N6 nanofiberfilter, neutralized polydispersed sodium chloride aerosols generated by a sub-micron aerosols generator (SMAG, model 7388L, MSP Corp., Shoreview, MN) was used in the loading to simulate accelerated loading under steady-state condition. The schematic layout of the SMAG for loading is depicted in *Figure 2.5*.

Sodium chloride solid, NaCl(s), was dissolved in deionized water to form an aqueous solution, NaCl(aq). Particle size distribution varied in accordance to the concentration of NaCl(aq) being used, ranging from 0.1% to 5%. Increase in solution concentration in the atomizer shifted the distribution curve towards the larger particle diameter. Saleem and Krammer has investigated the effects of dust concentration on a bag

filter under constant face velocity, the cake resistance and cake density are higher but the filter has a longer filtration cycle at lower dust concentration. They concluded that the influence of dust concentration is not significant on microfiber filter(M. Saleem, G. Krammer, 2007). However, the size effect of feeding particles on the filtration is proved to be more significant when the particles and fiber sizes are decreased, especially when the size of nanofiber and the nanoparticle are similar, due to the attraction force by Van der Waals force (Sumit S.R., Suman S.R., A.L. Yarin, B. Poudeyhimi, 2015). Therefore, the characteristics of aerosols could affect the loading behavior and mainly the properties of the cake formed during loading.

Under continuous supply of 0.2MPa compressed air into the atomizer, NaCl(aq) solution was atomized into submicron particles between 50 and 1000nm. This concentrated aerosol stream was further mixed with the compressed air (free of aerosol) forming the final aerosol stream that challenged the test filter. The flow rate and concentration of the aerosol stream were adjusted by further mixing with dilution air. The mixed polydispersed NaCl aerosol stream was dried by flowing through the Nafion membrane, a copolymer that removed moisture from the gas stream by pervaporation. The latter was driven by water content gradient between the gas streams flowing respectively inside and outside of the membrane. The dehumidified aerosol stream then flowed through the impactor with a 90° bend where large particles, due to inertia got captured by impaction with the plate and got removed. The particle cut

size (or diameter) depended on the impactor diameter as well as the aerosol flow rate. The remaining particles were directed to an electrical neutralizer where high-concentration air ions, generated by the electrical neutralizer, brought the incoming aerosol to a Boltzmann charge distribution. The polydispersed aerosol stream was fed subsequently to load-up the test filter mounted downstream in the test column with filter surface oriented perpendicular to the incoming flow. The face velocity was controlled by mixing the aerosol stream with a dried, cleaned make-up air flow, sourced from compressed air after passing through an oil removal filter and a submicron particle removing HEPA filter. Throughout the loading process, pressure drop across the filter was monitored by a digital pressure manometer (model 2080P, Digitron, Elektron Technology, UK) and the flow ratewas measured by a flowmeter (TSI-4100, TSI Incorporated, USA).

The purpose of isokinetic sampling(James P. Lodge, Jr., 1988) as mentioned in *Figure 2.5* is to capture the aerosols at the particular position and time without disturbing the flow pattern. This is done by monitoring and controlling the flow rate of the sampling tube, where the area is defined by the aera of the tube inlet, in order to keep the velocity of sampling inlet being the same as that of the main stream in the test chamber at that point.

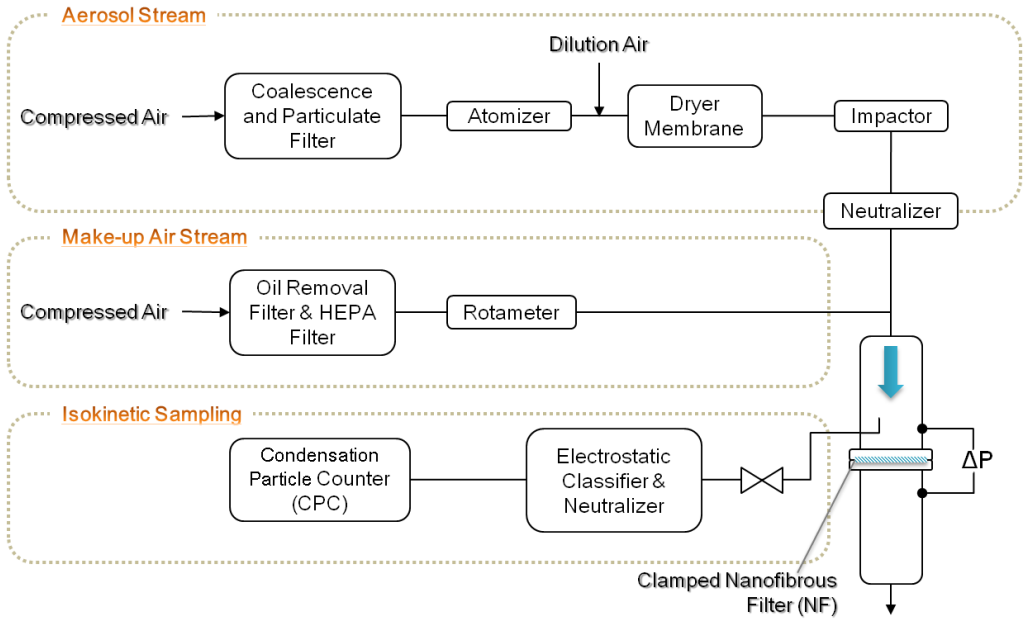

Figure 2.5The schematic of SMAG setup

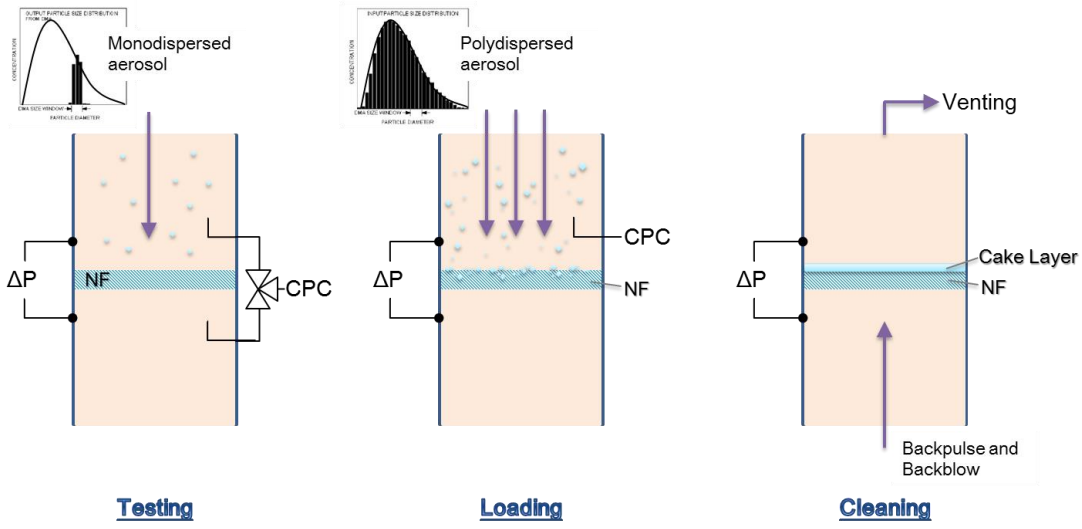

(a) (b) (c)

Figure 2.6The experiment setup of test column while (a)testing, (b)loading and (c)cleaning

After electrospinning, nanofiber sample produced first undergoes testing (see *Figure 2.6a*) on its pressure drop, filtration efficiency and quality factorat a given aerosol flow rate.

The single fiber efficiency (η_s) is

$$\eta_s = 1 - (1 - \eta(\mathrm{d}))(1 - \eta(\mathrm{imp}))(1 - \eta(\mathrm{int})) \approx \eta(\mathrm{d}) + \eta(\mathrm{imp}) + \eta(\mathrm{int}) \quad \text{Eq.(1)}$$

where$\eta(d)$, $\eta(imp)$ and $\eta(int)$ are the single fiber efficiency due to diffusion, inertial impaction and interception respectively.

Assume the filter has finite depth (L), by integration, the overall filtration efficiency (η) becomes(R.C. Brown, 1993)

$$\eta = 1 - \exp\left[\frac{-4\eta_s\alpha_f L}{\pi d_f(1-\alpha_f)}\right] \quad \text{Eq.(2)}$$

Quality factor, sometimes called figure of merit, of a filter is

$$\mathrm{QF} = \frac{-\ln(1-\eta)}{\Delta P} \quad \text{Eq.(3)}$$

Here, the aerosol stream was passed through the electrostatic classifier and neutralizer before sending to the test filter so that the air stream consisted of only monodispersed aerosol of a desired known

particle diameter. The filtration efficiency was determined by counting the particle concentration,respectively,upstream and downstream of the filter for efficiency. The monodispersed aerosol concentration was extracted from the polydispersed particles which depends on the NaCl solution concentration used, says 2%, the actual particles concentrations were $6.7\ (\frac{10^4\#}{\text{cc}})$, $19.6(\frac{10^4\#}{\text{cc}})$ and $1.6\ (\frac{10^4\#}{\text{cc}})$ for particle diameter of 50nm, 100nm and 300nm respectively.A three-way valve was installed before the condensation particle counter (CPC, model 3010,TSI Inc., Shoreview, MN) during testing to facilitate switching back-and-forth between measuring aerosol concentration in the air stream upstream and downstream of the filter, respectively. On the other hand, polydispersed aerosol was used for loading the filter (see *Figure 2.6b*) and the particle size distribution was measured by upstream sampling probe connecting to the condensation particle counter.

For cleaning (*see Figure 2.6c*), the setup was modified and the flow direction was reversed with venting at the top of the test column wherein the exhaust stream at the top vent collected the aerosols removed from the loaded filter.The regeneration was composed of a series of short-duration backpulses followed by continuous airflow or backblow. Due to the fragility of nanofibers, instead of a single air jet concentrating at one “spot”, the clean air passed through a tri-nozzle setup distributing three air jets targeted at the backside of the loaded nanofiber filter.*Figure 2.7* shows some possible designs of tri-nozzle setup, and (c)

was finally adopted for the test setup based on simplicity in design and the superior control in delivering three uniform rate jets. The tri-nozzle design further reduced the localized cleaning problem encountered by using a single nozzle as well as minimizing the local concentrated jet (backpulse and backblow) effect directed at the centerof the filter that can break the nanofibers there.

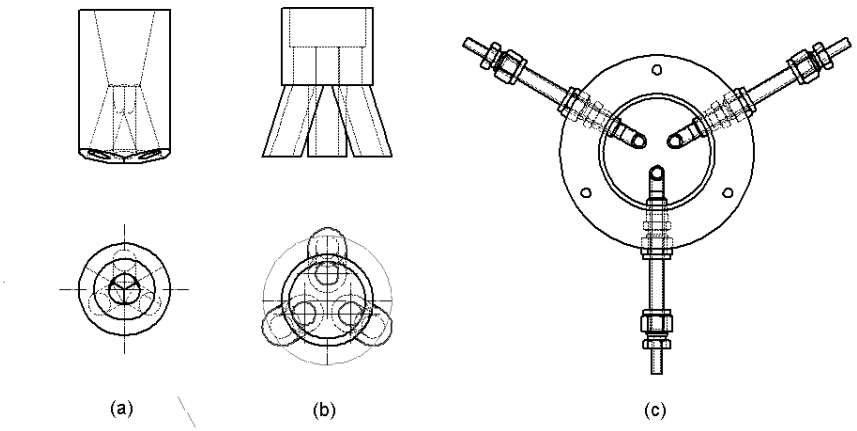

Figure 2.7Examples of tri-nozzle setup

2.3. Technology of Regeneration

Backpulse (BP) and backblow (BB) refer to clean air flowing from the backside or downstream side (from perspective of aerosol loading) of the filter media in pulsating mode and constant-flow mode, respectively. The schematic setup of cleaning is depicted in *Figure 2.8*. The overpressure to the filter media for cleaning directly depends on the

applied pressure of the compressed air source. Clean air blows from the downstream side of the filter sample through a solenoid valve and a nozzle, before reaching the backside of the preloaded filter. The settings of backpulse and backblow correspond to the open and close duration of the solenoid valve, respectively, which is controlled by a Programmable Logic Control (PLC) under sharp and fast response, where a ladder diagram was manually written before testing. The nozzle provides a venturi effect on the incoming jet-pulse.

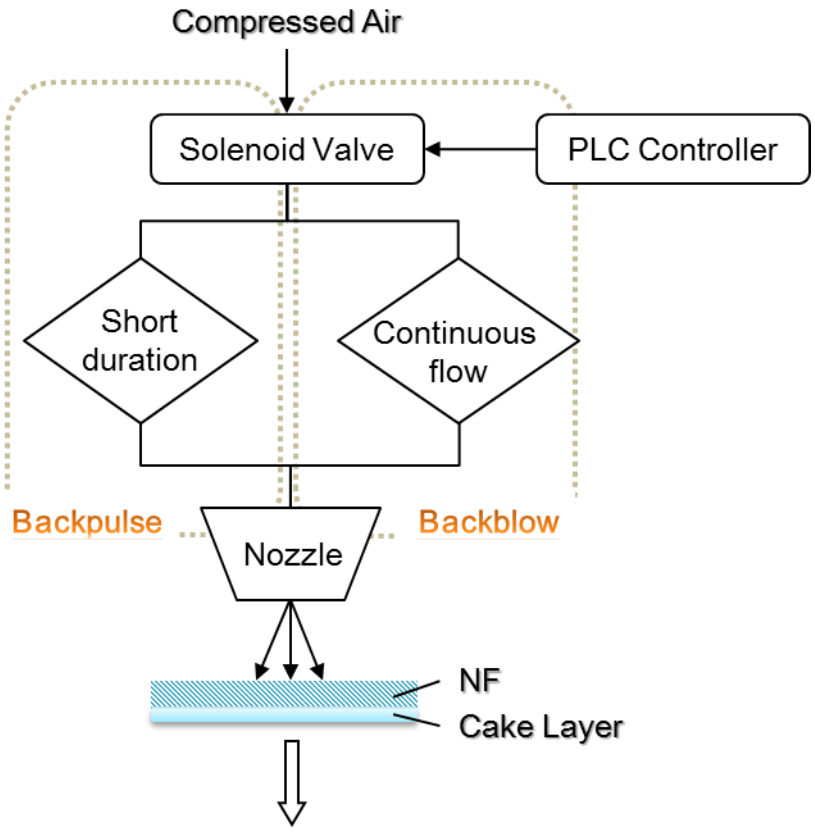

Figure2.8Schematic setup for backpulse and backblow regeneration

The jet duration, idle duration, blow duration and number of pulses in a series are pre-set in the ladder diagram with counters and timers. The working logic for backpulse and backblow are depicted in *Figure 2.9(a) and Figure2.9(b)*, respectively. Note that the pressure drop shown is actually an indication of input on/off signal to the solenoid valve, thus it is written as a sharp change.In actuality, backpulse and backblow have different cleaning mechanisms on the loaded filter. They can be combined to obtain synergistic effect on cleaning. The working logic of combining backpulse and backblow is depicted in *Figure 2.9(c)* where a series of pulse jets is executed before a constant airflow for backblow. Such “cycle” is repeated for the cleaning process. Beside the open and close duration of solenoid valve which controls the duration of backpulse and backblow, the number of backpulses before starting backblow is also a parameter to be optimized.

(a)

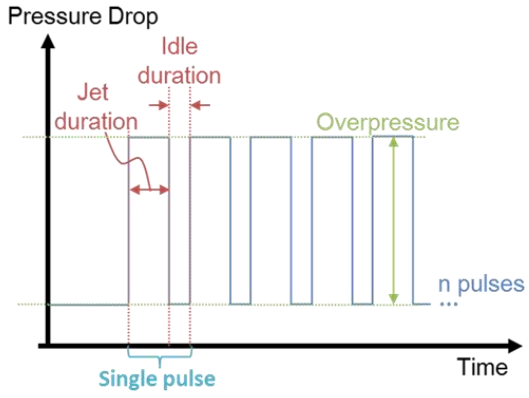

(b)

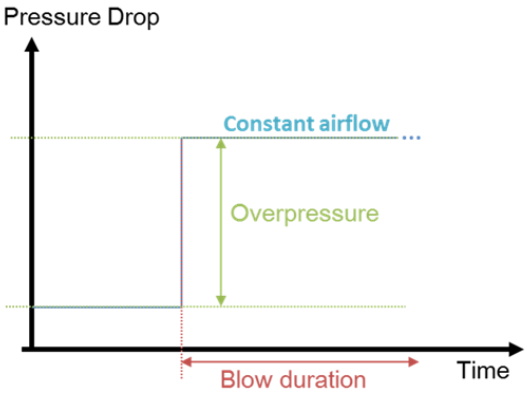

(c)

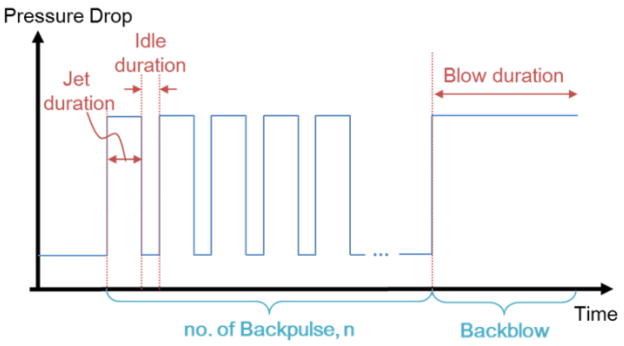

Figure 2.9The work logics of (a)backpulse, (b)backblow and (c)combined backpulse and backblow

Chapter 3

BASIC IN CLEANINGSINGLE LAYER NANOFIBER FILTERS

3.1. Filter Properties

An electrospun single-layer nanofiber filter is made up of a layer of nanofiber mat (despite of the thickness where nanofibers are stacked together as a single-layer nanofiber filter)in which the nanofibers are collected by a spunbond substrate during electrospinning. The substrate subsequently also serves as supporting material to the nanofibers. It is the simplest configuration of a single-layer nanofiber filter.

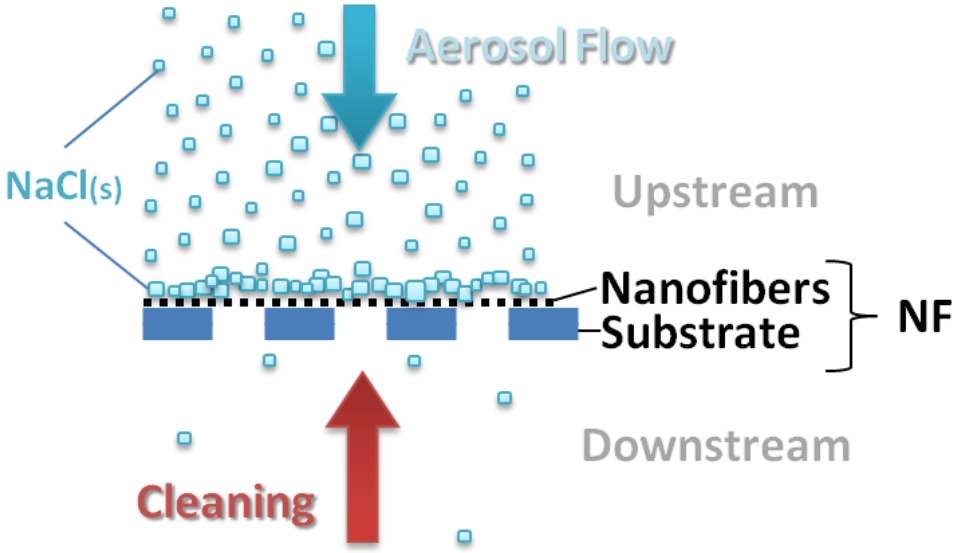

Figure 3.1 Conceptual picture of loading and cleaning single-layer nanofiber filter

The properties of the substrate were tested and examinedwith general testing procedures of testing a filter media (See *Section 2.2*),

and proved to have no contribution to filtration or loading process for its negligible pressure drop and filtration efficiency in our laboratory. During loading or filtration testing, the nanofiber mat is facing upstream as delineated in *Figure 3.1*.

It is worthy to note that the adhesion between nanofiber mat and substrate highly depends on the material properties of the substrate. For conventional spunbond nonwoven polypropylene substrate, the adhesion of the nanofibers to the substrate is not sufficientlystrong to withstand the backpulse and backblow cleaning,and the nanofibers can get damaged by the high-speed airflow and pulsejet targeted at the backside of the filter tearing the nanofiber mat from the substrate. Surface treatment (e.g. hydrophilic treatment) on substrate material (F . Rombaldoni, K. Mahmood, A. Varesano, M.B. Songia, A. Aluhi, C. Vineis, G. Mazzuchetti, 2013)can increase the wettabilitythereby improvingthe attachment of nanofibers onto the substrate.

There are two typical cases of nanofiber failure during cleaning. *Figure 3.2(a)*demonstrates the pressure drop after cleaning being lower than the initial pressure drop of a clean filter before loading (i.e. ΔP_f). This results in negative residual ratio (i.e.$\frac{\Delta P_r - \Delta P_f}{\Delta P_o - \Delta P_f}$) indicating that a serious damage has been made on the nanofiber mat. Another one is abnormal increase in pressure drop during cleaning, see *Figure 3.2(b)*, which is caused by scratches made on the nanofiber layer and at certain location of scratches the nanofibersareactually detached from the

substrate. The peeled off nanofiber layer enhancesat times the resistance of the entire filter and at other times behavesjust normally. This is due to the flexibility of nanofibers without the support of the substrate. Due to the fragility of the nanofibers, therefore a better adhesion between nanofibers and substrate is highly desirable.

(a)

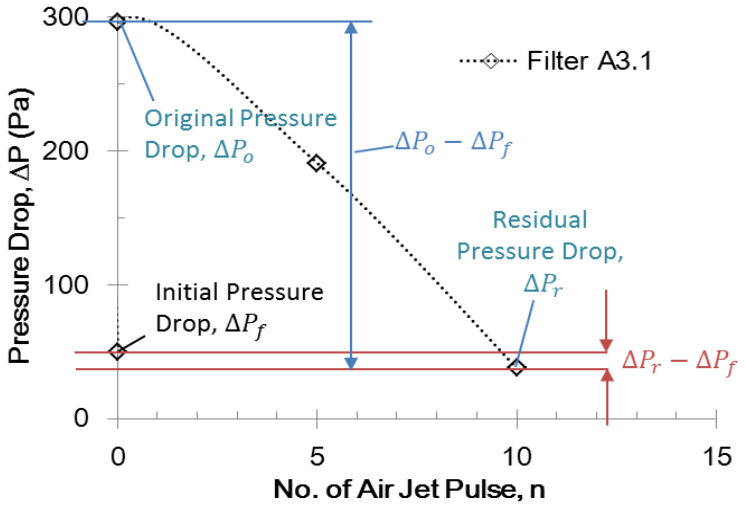

(b)

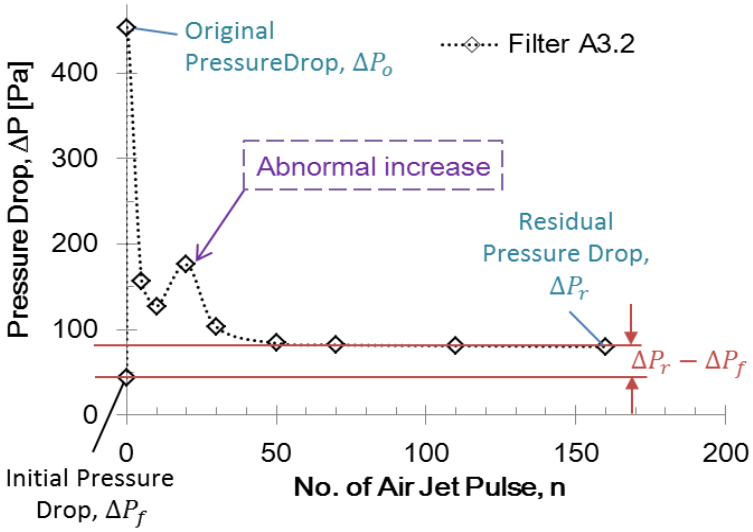

Figure 3.2Examples of abnormal cleaning behaviourobtained from our testing due to (a)damage and/or (b)scratches made on the nanofiber layer

3.2. Filter Configurations

The thin nanofiber is weak and cannot withstand the high jet velocity from the high overpressure applied upstream during the cleaning process and thus the cleaning is ineffective due to use of a much lower velocity jet to avoid nanofiber damage. Essentially the jet targeted at the backside of the filter pushes the nanofiber mat tearing it away from the substrate. The nanofibers can break easily in the filter during backpulse and backblow cleaning due to the insufficient adhesion between substrate and nanofiber layer. Four filter configurationshave been investigated and they are depicted in *Figure 3.3*.

Filters A and D are the simplest filter configuration, including only nanofiber and its supporting substrate. Conventional spunbond polypropylene substrate was used for Filter A while substrate that hasundertaken surface treatment was used in Filter D.

Filter B is asample where the adhesion between conventional substrate and nanofiber layer is strengthened by adding adhesive at the interface. To minimize the blockage of airflow across the filter, adhesive material is sprayed onto the substrate before undergoing electrospinning.

On the other hand, the nanofiber layer in Filter Cis being sandwiched between two conventional substrate layers in which the upstream substrate is added after electrospinning and before loading

and cleaning to provide extra support to the nanofibers during backpulse and backblow cleaning.

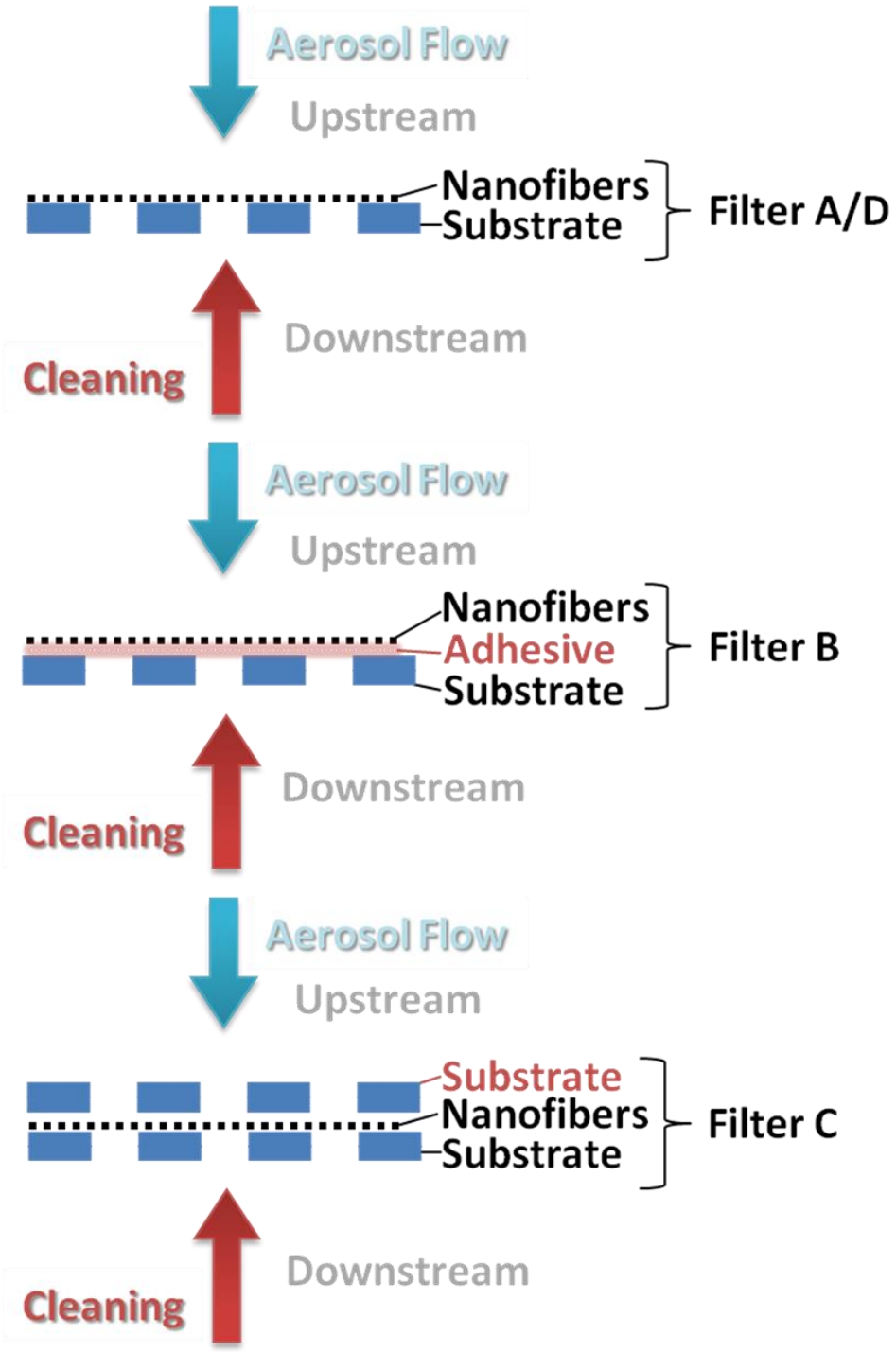

Figure 3.3Conceptual drawing of filter configuration during loading and cleaning

In the experiment, the filtration efficiency η for a given particle size was obtained from using the differential mobility analyser (DMA) to classify other particle size ranges allowing only the particle size $D_p$to challenge the filter. The filtration efficiency is given by

$$\eta = 1 - \frac{C_d}{C_u} \qquad \text{Eq.(4)}$$

where C_d and C_u are the downstream and upstream concentration of a given particle size, and of course η, $C_d$and $C_u$are functions of D_p. ηhas also been referred as the grade efficiency as it depends on the aerosol size D_p. The pressure drop across the filter ΔP was also measured, and the QF can be determined from Eq. (3).

The filtration efficiencies, quality factorsand properties of clean Filters A to D are depicted in *Figures3.4(a), Figure 3.4(b)* and *Table 3.1* respectively, and all tests wereconducted at a face velocityof 5.3cm/s. In *Figure 3.4(a)*, the efficiency has a V-shape when plotted against the aerosol size. This is due to the fact that for aerosol size less than 100nm, the capture is mainly by diffusion whereas for aerosol size greater than 100nm, the capture is mainly by interception. These two mechanisms dominate the capture for nano-aerosols. The aerosol size corresponding to the minimum efficiency is referred as the most penetrating particle size (MPPS). All four filters have this characteristics V-shape behaviour, with some behave more so than others.

Filters A to C were electrospun under the same electrospinning conditions and the properties of nanofibers are assumed to be the same. However, since Filter D has smaller mean fiber diameter due to the higher electric conductivity of substrate used, the results of Filter D cannot be compared directly with the rest of samples.

		Adhered	**Sandwiched**	
	Filter A	Filter B	Filter C	Filter D
Mean fiber diameter, $\mathbf{d_f}$ (nm)	220	220	220	180
Pressure drop of clean filter, $\Delta\mathbf{P_f}$ (Pa)	23	30	23	24
Filtration efficiency, $\boldsymbol{\eta(100nm)}$	52.8%	61.6%	51.7%	63.7%
Filtrationefficiency,$\boldsymbol{\eta(300nm)}$	62.5%	70.7%	59.6%	68.7%
QualityFactor $\boldsymbol{QF(100nm)}$ $\boldsymbol{(10^{-2}Pa^{-1})}$	3.33	3.21	3.22	4.22
Residual Ratio	N/A	0.38	0.26	0.12
Substrate	Conventional spunbond polypropylene			Hydrophilic spunbond polypropylene

Table 3.1 Filter properties of different filter configurations

As the substrate material provides neither filtration efficiency nor media resistance, the sandwiched sample, Filter C, has similarbehaviour as Filter A. Beside, Filter B results in higher filtration efficiency and pressure drop due to the added adhesive, yet there is not much deviation onthe quality factor betweenFilter A and Filter B implying the filter properties of both filters are similar. From the efficiency curves in *Figure 3.4(a)*, the MPPS is approximately 120nm for nanofiber filters with mean fiber diameter in the range of 180nm to 220nm while the MPPS of microfiber filters are normally about 300nm

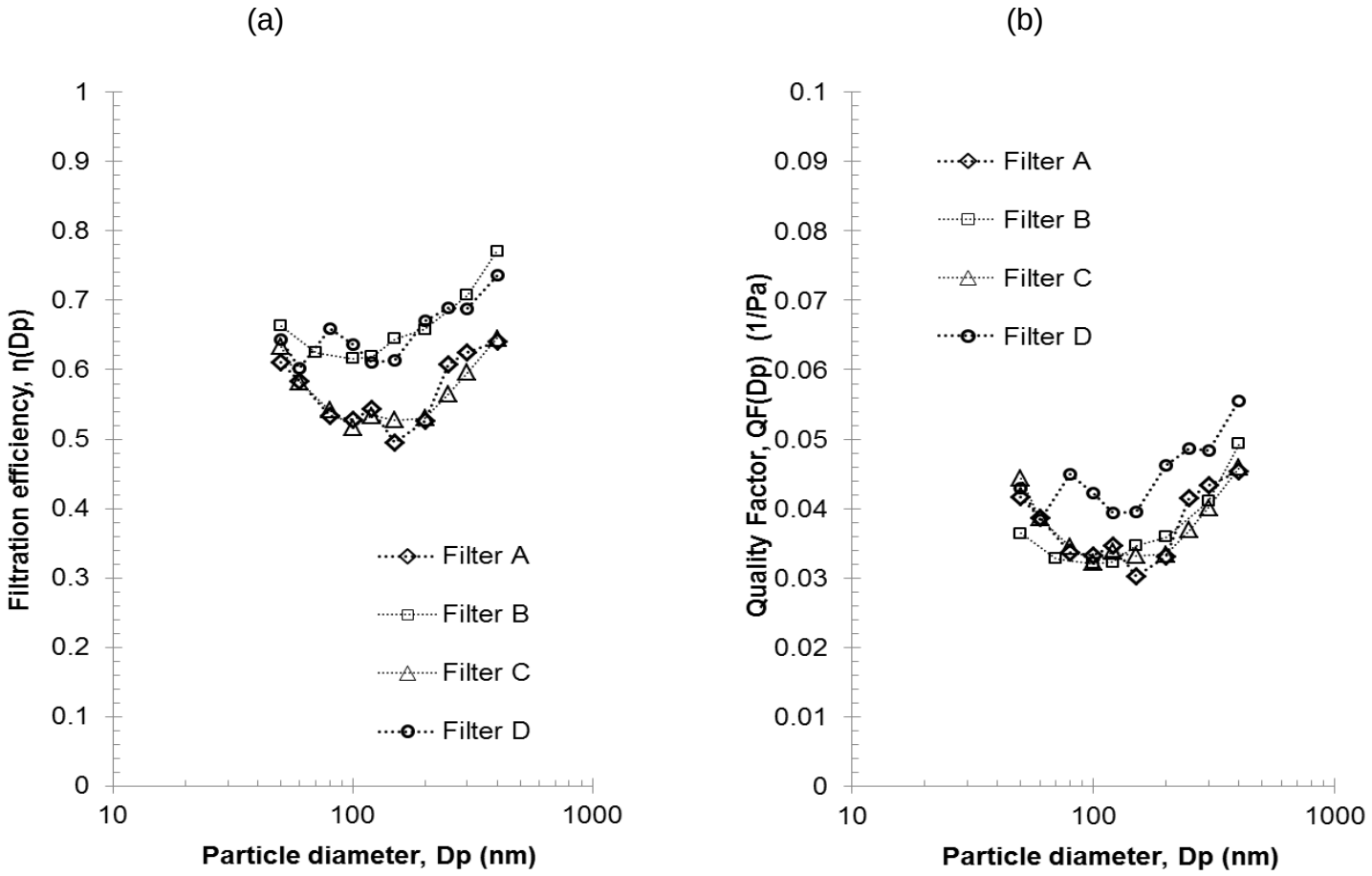

Figure 3.4(a)Filtration efficiencies and (b)quality factors of different filter configurations

Moreover, owning to the fact that Filter A cannot withstand the high pressure applied, the overpressure cannot reach theminimum threshold, i.e. the critical value, for cleaning. Therefore, the cleaning is ineffective,thus the results of Filter A have been discarded. On the other hand, the results of Filter D have beenchosen to be presented in the following because it has the simplest configuration, unlike Filter B that has additional adhesive and unlike Filter C that has additional upstream substrate that hampered cleaning. Both artifices can lead to uncertainties in the cleaning outcome.

3.3. Three-stage-cleaning

In this section the general regeneration behaviour of a filter will be discussed.Despite of variations in filter samples, loading and cleaning settings, the regeneration behaviours are all similar. There are three characteristic stages of regeneration. First, there is a very rapid cleaning process that removes most of the deposited particles, thus the pressure drop decreases precipitously. The second stage is a transition between the first rapid cleaning stage and the final ineffective cleaning stage. In the second stage, the remaining particles are more difficult to be removed and this involves particles migration dislodging from one location and attaching possibly to the filters further downstream of the cleaning flow. This seems to be a time-dependent process, therefore the

pressure drop decreases slowly over time. Finally, when the regeneration reaches the third stage, the pressure drop remains nearly constant with further backpulse or backblow. This indicates that no more trapped particles can be removed and the pressure drop reflects the trapped residual solids remaining in the filter; this is also referred as the residual pressure drop after cleaning.

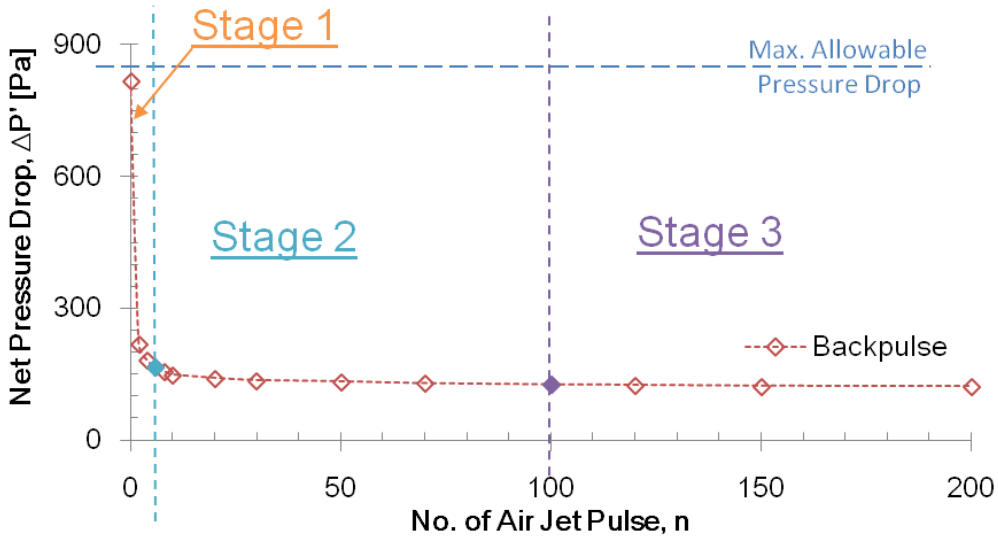

Figure 3.5 Example of three stages of cleaning in nanofiber filters[d_f =180nm]

*Figure3.5*shows an example on the cleaning behaviour. The filter was loaded with aerosols under steady condition to the maximum pressure drop of 840Pa. Once the pressure drop reached this maximum level, loading was stopped and filter cleaningwas initiated.The test filter sample shown in *Figure 3.5*was cleaned by backpulse, where the

netpressure drop, $\Delta P'$,is the pressure drop after subtracting the clean filter pressure drop, ΔP_f, i.e.$\Delta P' = \Delta P - \Delta P_f$.

The three stages are generally defined as follows:

Stage 1: $$\left|\frac{d\,(\Delta P')}{dn}\right| \geq 30\ \text{Pa} \qquad \text{Eq. (5)}$$

Stage 2: $$0.1\text{Pa} < \left|\frac{d\,(\Delta P')}{dn}\right| < 30\ \text{Pa} \qquad \text{Eq. (6)}$$

Stage 3: $$\left|\frac{d\,(\Delta P')}{dn}\right| \leq 0.1\ \text{Pa} \qquad \text{Eq. (7)}$$

As for backblow, the three stages are defined as follows:

Stage 1: $$\left|\frac{d\,(\Delta P')}{dt_b}\right| \geq 30\text{Pa/s} \qquad \text{Eq. (8)}$$

Stage 2: $$0.1\ \text{Pa/s} < \left|\frac{d\,(\Delta P')}{dt_b}\right| < 30\ \text{Pa/s} \qquad \text{Eq. (9)}$$

Stage 3: $$\left|\frac{d\,(\Delta P')}{dt_b}\right| \leq 0.1\text{Pa/s} \qquad \text{Eq. (10)}$$

3.4. Backpulse and Backblow in Nanofiber Filters

To investigate the effect of backpulse and backblow in cleaning loaded nanofiber filter, two experiments were carried out separately. In both cases, the filter was loaded under face velocity of a 5.3cm/s with polydispersed aerosols with sizes in the range of 50nm to 500nm at an aerosol concentration of 0.00294$\mathrm{g/m^3}$until the pressure drop reached the arbitrary set maximum allowable pressure drop, 840Pa. The loaded filter then underwent cleaning with an applied pressureof 6.5bar, using tri-nozzle setup. In one case, the loaded filter was cleaned with backpulse only. In another case, the loaded filter was cleaned with backblow only. The mean fiber diameter of each samplewas measured to be 180nm with the clean filter pressure drop of 30Pa at a face velocityof 5.3cm/s.

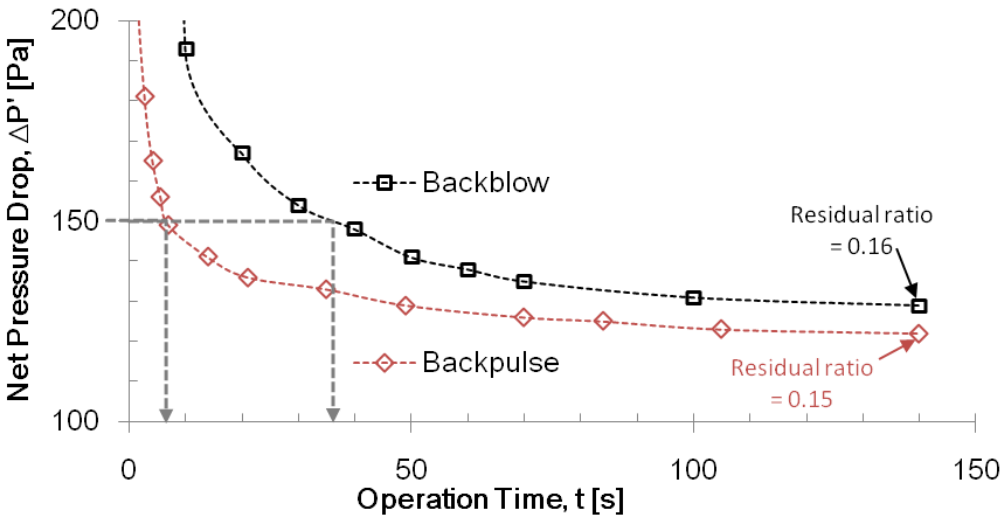

Figure 3.6Cleaning curves of two preloaded nanofiber filters cleaned, respectively, with backpulse and with backblow only[d_f=180nm]

To compare the effectiveness, the cleaning curves are plotted with pressure drop against operation time in *Figure 3.6*. For backpulse, each single pulse with a duration of 0.7s consisted of 0.5s jet pulse and 0.2s of idle. For backblow, a time interval based on 10s was set in order to ensure the valve opening time is sufficiently long to develop steady air flow. Hence, the number of timesof pressure drop measurement was minimized to reduce the effect of jet-similar impact on the filter which involves disruption and interruption to the cleaning process.

Before discussing the results, it is useful to quantify the cleaning effectiveness using a residual ratio. Residual ratio is a convenient indicator, or indirect measure,of the percentage of solids residing in the filter after cleaning. It is defined as the ratio of residual ∆Pminus the clean filter ∆P, to theloaded filter ∆Pminus the clean filter ∆P, as given *Equation (11)*.

$$\text{Residual ratio} = \frac{\Delta P_r - \Delta P_f}{\Delta P_o - \Delta P_f} = \frac{\Delta P'_r}{\Delta P'_o} \qquad \text{Eq. (11)}$$

In the comparative experiment, also from *Figure 3.6*, after 2.3 minutes of cleaning, when the cleaning reached stage 3, the residual ratio was determined to be 0.16 for the case of backblow only, and 0.15 for backpulse only. Cleaning a loaded filter with backpulse has shown to be slightly more effective than backblow over time. While the end points reached by the two methods were not too far different, the time to attain a desired residual pressure drop is quite different. For example, for a

desired pressure drop of 150Pa, the time needed for backpulse is only 6s while for backblow cleaning 36s, which is 6 times more. Therefore, backpulse is a faster and more efficient cleaning process than backblow.

In the experiments discussed in the foregoing paragraphs, the cleaning effectiveness of backpulse and backblow were compared revealing backpulse being better than backblow. However, the filter media is cleanable by either of the two approaches and the difference between the results indicates that the cleaning mechanism for both may be different.

To that end, further experiments were carried out to investigate the cleaning behaviour of a loaded filter cleaned by combined backpulse and backblow, and the result is compared with that of a filter cleaned by backpulse only in *Figure 3.7*. In the experiment, there were 10 pulses in a series of backpulses (i.e. n=10), for which each single pulse consisted of 0.5s jet pulse followed by 0.2s of idle. After the 10 backpulses, there was 10s of backblow. This “cleaning cycle” was repeated. The backpulse setting for the backpulse mode only was the same as with the backpulse in the combined mode.

In terms of efficiency, cleaning by beackpulse is better as the time spent in cleaning is minimized. On the other hand, the result shows that the combined backpulse and backblow has better effectiveness with residual pressure drop further minimized. The residual ratio dropped

down to 0.11 for the combined regeneration, which is lower than 0.15 for backpulse cleaning.

In stage 2, the cleaning changes from effective to relatively ineffective for backpulse only as shown in *Figure 3.7*. Despite cleaning by backpulse has shown a very rapid cleaning initially, combined regeneration has given a more stable particle removal in stage 2.Finally, in stage 3, from the slopes drawn with the pulses at beginning of stage 3, combined regeneration also showed higher rate of particle removal. In short, cleaning by backpulse alone reaches the saturated residual pressure drop earlier than the combined cleaning. It is conjectured that by backpulse alone, the solids are detached by inertia impulses and some extent by shear yet the loosened solids get recaptured by the fibers further downstream. On the other hand, further with backblow, the detached solids may be carried out of the filter with lesser possibility of loosened solids being recaptured.

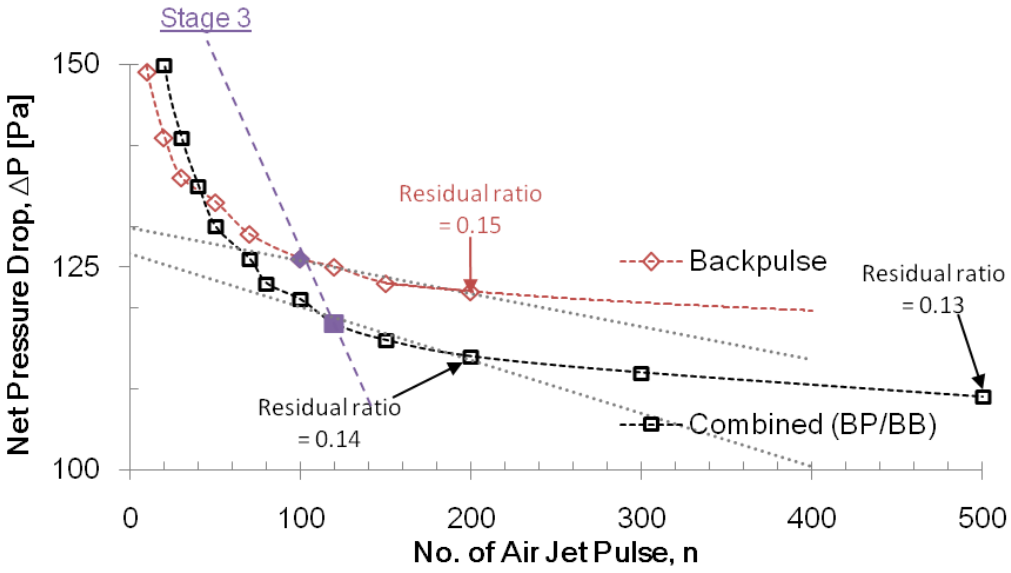

Figure 3.7Cleaning curves of nanofiber filter cleaned with backpulse only and with backpulse-followed-by-backblow.[d_f=180nm]

Chapter 4

INFLUENCE OF OPERATION PARAMETERS ON CLEANING PERFORMANCE OF NANOFIBER FILTERS

4.1. Jet Duration

It was suggested(S. LAUX, U. RENZ, 1993) that a sudden change of the overpressure is the unique factor in blowback cleaning and jet duration is not responsible for cleaning a conventional baghouse filter. Along this idea, the effect of jet duration of backpulse onthe cleaning effectiveness has beeninvestigated.

The experiments were carried out at a face velocity of 5.3cm/s with applied pressure 6.5bar using tri-nozzle setup. All these cleaning conditions were kept constant, except the backpulse jet and idle durations have been changed. There were three sets of backpulse settings representing three different valve response times respectively for drawing a comparison. They are fast, moderate and slow responses corresponding to 0.1s, 0.3s and 0.5s respectively. To modify the variations, the idle duration was set to be identical as the jet duration, which means for moderate valve opening time, the jet duration and idle duration were both 0.3s.

The results are shown in *Figure 4.1*. There were two sets of experiments carried out.One was cleaned by a combination of backpulse and backblow, while the other one was cleaned by backpulse alone. Results suggest that the longer jet duration has a better cleaning effectiveness. As mentioned in previous section, cleaning with backpulse and backblow results in lower residual ratio, this result is also depicted in this figure. Both experiments were stopped at 300th pulse (i.e. n=300) and the final pressure drop across the filter is taken as residual pressure drop.

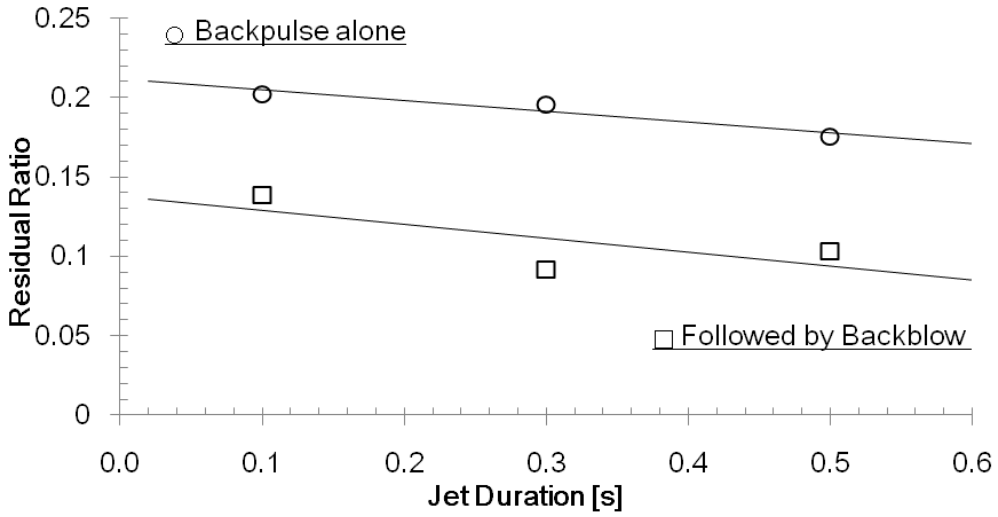

Figure 4.1Residual ratios of nanofiber filters cleaned by different jet duration[d_f =280nm]

The results indicatedthat the cleaning mechanism of backpulse is due to the sudden impact caused by the overpressure on the filter that causes a mechanical shock on the cake which breaks up the cake and the jet is able to remove the deposited solids. The valve opening time is not a critical factor but there exists a trend that a longer valve opening time can ensure the impact pulse acting more effectively on the fibers and to loosen the deposited solids from the filter.

Overall, to achieve better cleaning effectiveness, the combination of backpulse and backblow is adopted in the following experiments unless specified.

4.2. Applied Pressure

Another set of experiments was carried out to investigate the effect of applied pressure on nanofiber filter cleaning. The applied pressure is directly affecting the overpressure acting on the filter during the cleaning process, i.e. backpulse and backblow, whereas the overpressure is the major factor influencing the cleaning efficiency in conventional microfiber filter.

The loaded filters were cleaned by combination of backpulse and backblow at a face velocity of 5.3cm/s. The backpulse was composed of 0.5s pulse-jet and 0.2s idling. Ten backpulse pulses formed a backpulse series while the backblow duration was 10s, which followed soon after a complete series of backpulse.

The only variation in the experiments wasbeing the pressure ofthe compressed air tank, which assumed three levels - 3 bar, 4 bar and 6.5 bar respectively. The results are plotted in *Figure 4.2*. The residual ratio of filter cleaned with 3 bar, doubles that of 6.5 bar; while the case with 4 bar was between the two. This shows that the cleaning efficiency increases with the magnitudeof the applied pressure, similar to the case of conventional microfiber filter cleaning[15] [16] [17] [18].

However, it is worthy to note that there is an upper limit onthe applied pressure due to the fragility of nanofibers which depends on the fiber diameter, fiber mat thickness, adhesion between nanofibers and its

supportive substrate,and the cleaning setup configurations. The latter depends on the standoff distance of jet, single versus multi-jets, air velocity from each jet, uniformity and area coverage.No question that the tri-nozzle setup has made a single vigorous jet divided into three gentler jets providing a more uniform cleaning of the filter.

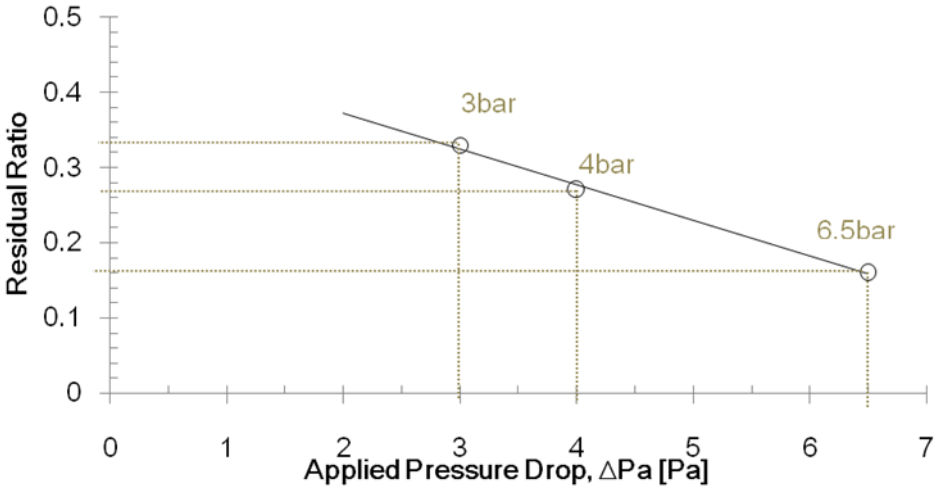

Figure 4.2Residual ratios of nanofiber filters cleaned by different applied pressure[d_f=180nm]

4.3. Mean Fiber Diameter

Experiments were carried out to investigate the effect of fiber diameter in cleaning apreloaded nanofiber filter. The pressure drop for the test filter at clean state prior to loading was 30Pa at a face velocity of 5.3cm/s. The fiber diameters for the 3 test filters were 120, 180 and 280nm. The cleaning method was series of backpulse followed by

backblow for 10s. The backpulse was composed of jet duration of 0.5s, idle duration of 0.2s, and 10 pulses as a series of backpulse. All the experiments were done under this cleaning setting.

The results in terms of residual ratio versus fiber diameter areshown in *Figure 4.3*. It is more difficult to remove the captured particles on a nanofiber filter with smaller mean fiber diameter due to the large surface area to volume ratio for which the particles are held tighter to the fiber surface from the Van der Waals attractive force.

Theparticle size distribution of the submicron aerosols used for loading is shown in *Figure 4.4.* It can be seen thatit is a lognormal distribution curve and the count median diameter is approximately 120nm. The attraction forces between 120nm diameter particles with comparable 120nm diameter nanofiber aregenerally greater than 120nm particles but with distinctly larger diameterfibers, such as, 180nm or 280nm.

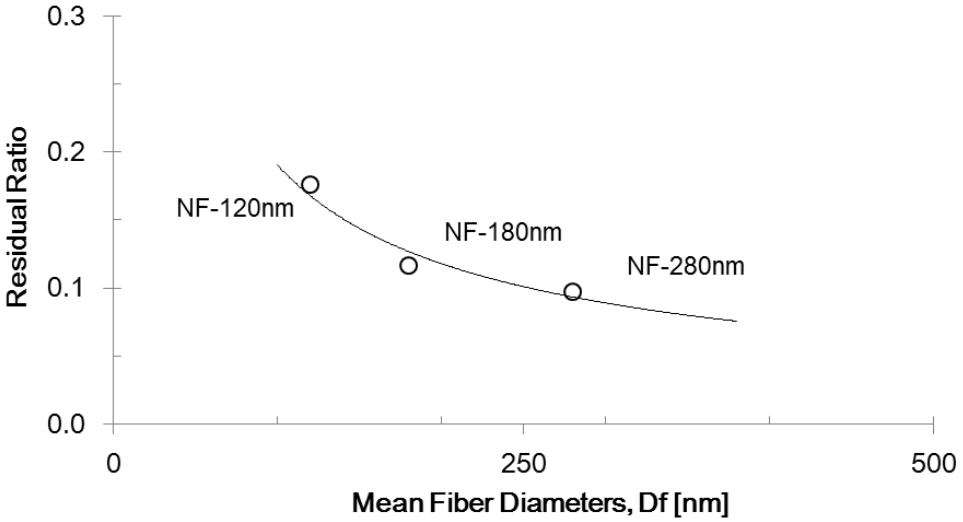

Figure 4.3Residual ratios of nanofiber filters with different mean fiber diameters

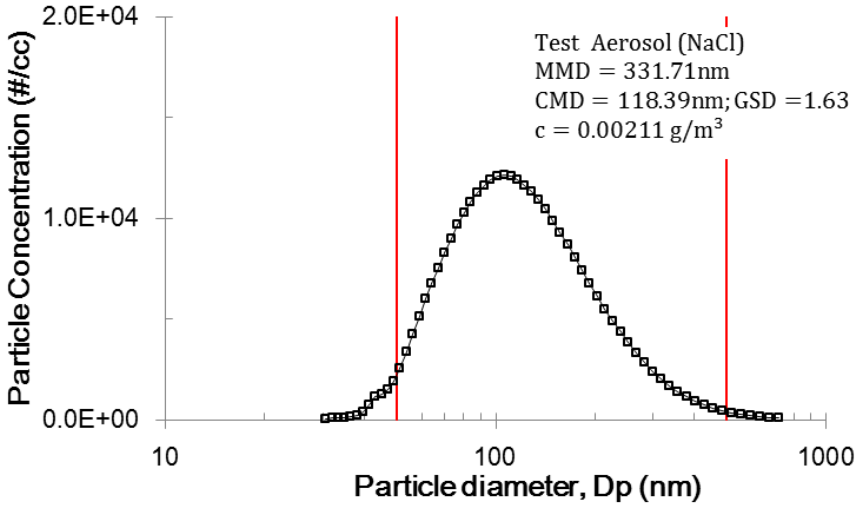

Figure 4.4Particle distribution curve for loading the nanofiber filters with different fiber diameters

4.4. Filter Thickness

By Davis correlation(W .W.F. Leung, C.H. Hung, P.T. Yuen, 2010), under same face velocity, the clean filter pressure drop (ΔP_f) is proportional to fiber matthickness (i.e. filter thickness) (Z) and also a function of the fiber packing density (α_f) for the same fiber diameterD_f.

$$\Delta P_f \sim f(\alpha_f) Z \qquad \text{Eq. (12)}$$

Assume that the increase in packing density due to the rise in fiber weight is negligible. Then,*Equation (8)* becomes:

$$\Delta P_f \sim Z \qquad \text{Eq. (13)}$$

The clean filter pressure drop (ΔP_f) which is also the initial pressure drop before aerosol loading is proportional to the filterthickness (Z) of the nanofiber filter with same fiber diameter.

In all the experiment, the cleaning was carried out with combination of backpulse and backblow with the same setting. The only variation was the filter thickness. The face velocity was 5.3cm/s. The jet duration, idle duration and backblow duration were 0.5s, 0.2s and 10s respectively. Ten backpulse pulses formed a backpulse series. The applied pressure was 6.5bar.

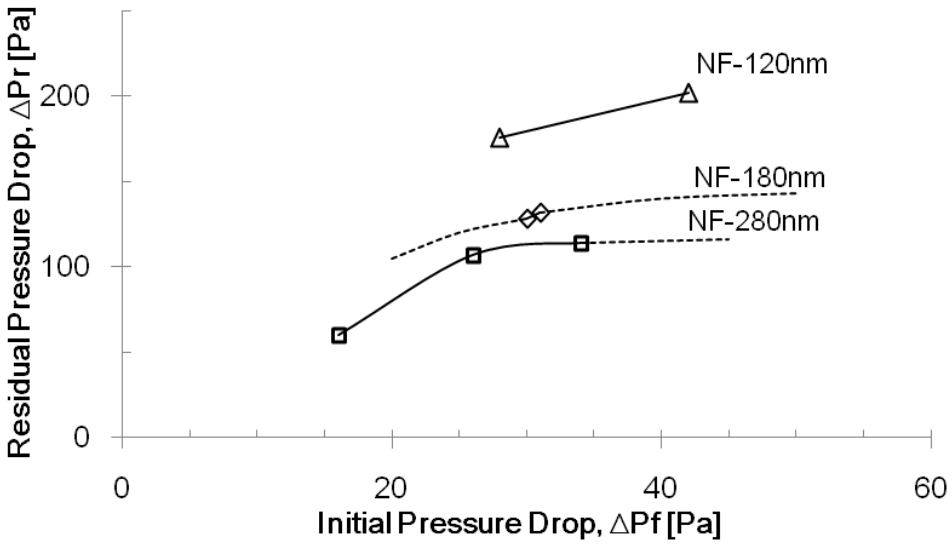

Figure 4.5Residual pressure drop of nanofiber filter with same fiber diameters but different clean filter pressure drop

The results in *Figure 4.5*show that the residual pressure drop increases with initial pressure drop thus also the nanofiber mat thickness. This is due to increase in recapture of the loosened particles inside the filter mat for a thicker filter. Unfortunately, increasing the fiber mat thickness, which also increases the dust holding capacity, alsoincreases the residual pressure drop. However, the relationship between fiber mat thickness and the dust holding capacity (and residual pressure drop) is not linearbecause of the skin effect as the loading across the fiber mat thickness is not uniform. Therefore, it is desirable not to have a very thick nanofiber mat due to (1) increase in capacity may be reduced by skin effect, and (2) regeneration of a preloaded filter is more difficult due to increase in recapture of loosened aerosols.

Chapter 5

CYCLIC CLEANING ON SINGLE LAYER AND MULTILAYER NANOFIBER FILTER

5.1. Single Layer

From previous studies, nanofiber filters have demonstrated to be cleanable. The next step is to investigate the behavior of cyclic loading-and-cleaning of a single-layer nanofiber filter. Experiments were carried out as illustrated in the schematic of *Figure 5.1*.

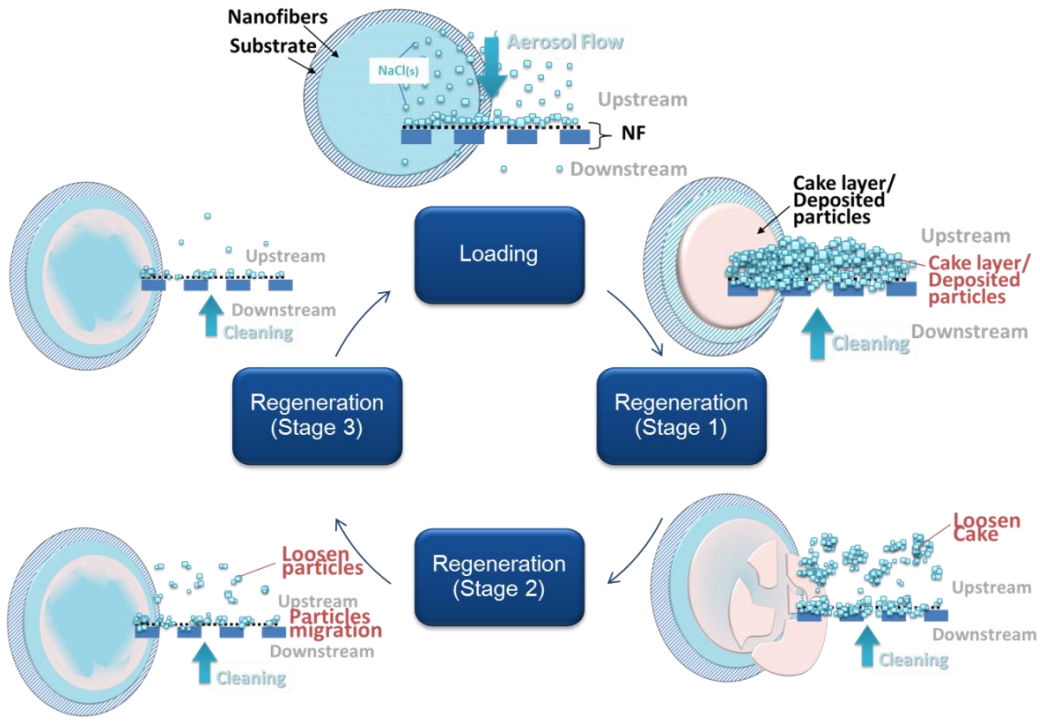

Figure 5.1Schematic picture of filtration cycles

The filter was mounted inside the test column. Neutralized polydispersed sodium chloride aerosolswith sizes in the range of 50nm

to 500nm at an aerosol concentration of 0.00294g/m^3generated by a sub-micron aerosol generator was fed,at a face velocity of 5.3cm/s, into the test chamber to perform an accelerated loading test under steady condition.The cleaning was triggered at the arbitrary set upper limit pressure drop of 850Pa. Backpulse and backblow were carried out with a tri-nozzle setupwith clean airflow in reverse direction, from the downstream side of loading. All cleaning used applied pressure of 6.5bar. The duration of pulse-jet, idle, and backblow were 0.5s, 0.2s and 10s, respectively.

Throughout the experiment, pressure drop across the filter and the flow rate were monitored by a digital pressure manometer and a flowmeter,respectively.The filtration cycle (i.e. loading followed by cleaning) had been repeated several times (i.e. number of filtration cycles, N).

The results revealed that the cleaning behaviors were similar fordifferent cycles with the three stages of cleaning, a steep decrease in pressure drop across the filter due to the removal of cake, a modest decrease as a transition between first and final stage of loosened aerosols in the filter, and finally a slow decrease where remaining aerosols firmly adhered to or trapped inthe nanofiber filter were hardly removed by the airflow.

Once the cake is removed in the first stage, in the second and third stage aerosols trapped inside the filter are detached from upstream of the filter in the direction of cleaning flowby inertia and/or by shear and during the course of convection some aerosols get recaptured at the further downstream of the filter while others get blown off from the filter. The trapped aerosols mostly at the downstream end of the filter further narrow down the flow passage resulting in higher pressure drop of the filter. This further boosts up the skin effect at the upstream end of the filter during loading. This is represented by $\Delta P_{r,1}$ - ΔP_f in *Figure 5.2*.

The test nanofiber filter underwent several loading-cleaning cycles until the sixth cycle, cracking was found and the experiment was stopped. The pressure drop measurements for the entire 6 cycles are depicted in *Figure 5.2.*As can be seen, the residual pressure drop was increasing with increasing cycles and the filtration cycle time of subsequent cycles are reduced (almost by half) as compared to the first long cycle.

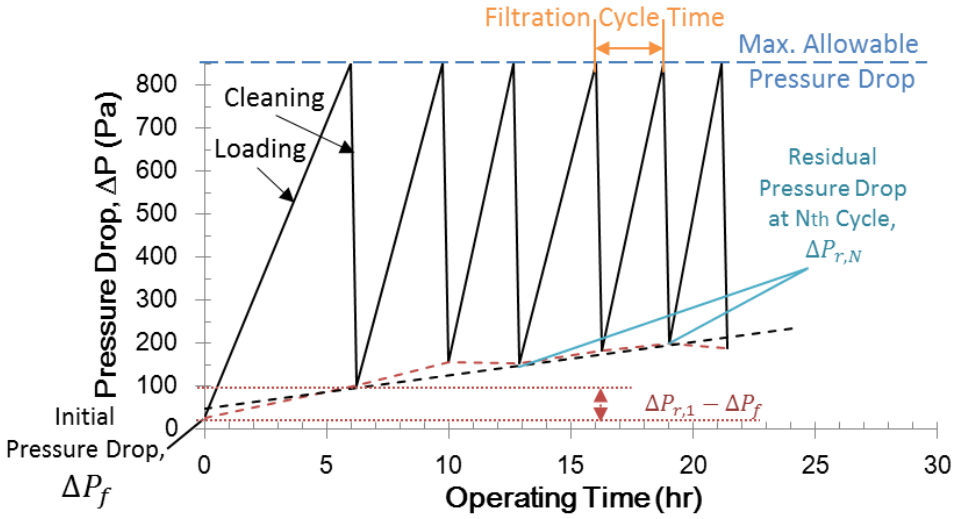

Figure 5.2Pressure drop with operating duration of nanofiber filter for filtration cycles, i.e. loading and cleaning[d_f=280nm]

A closer examination on the characteristic of residual ratio and the cycle duration are shown in *Figure 5.3*. The sample has demonstrated a stable behaviorwhere the growth in residual pressure drop and the decreasein filtration-cleaning cycle durationtake place mainly inthe first filtration-cleaning cycle.These two variables stay constant thereafter thefirst cycle, i.e. the conditioning phase (VDI 3926). Specifically, the filtration cycle time from first to second cycle was decreased by half while the residual ratio was increased from 0.092 to 0.157, a 1.7 times increase. From the secondto sixth cycle, the residual ratio started increasing slowly from 0.157 to 0.197 for five consecutive cycles, while the cycle duration was approximately constant in the range of two to three hours.

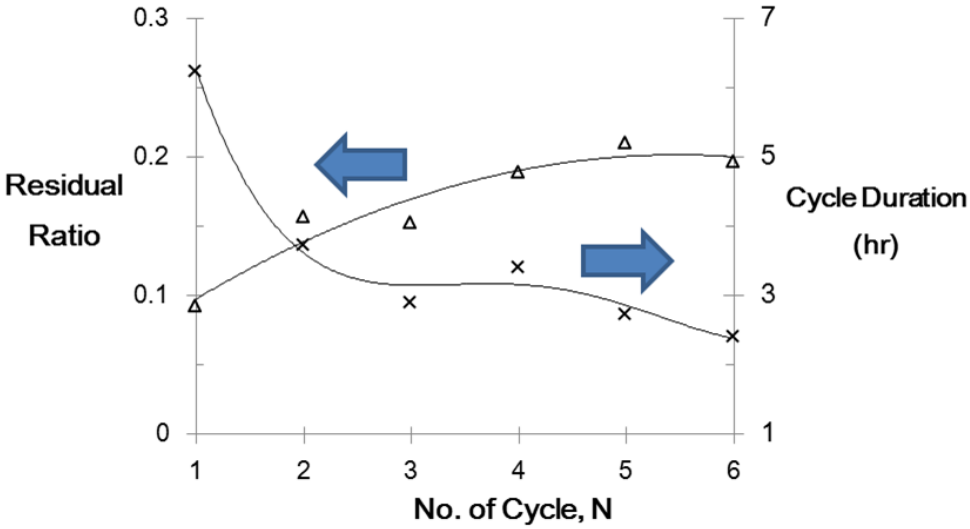

Figure 5.3The characteristic of residual ratio and the cycle duration at each cycle

Interestingly, the loading behavior was convex-upward in shape for thefirst cycle (and at times linear), but became concave shape in the subsequent cycles as shown in *Figure 5.4*.

For a clean nanofiber filter, there are both open and dead pores in the filter. “Open pores” are pores that can be easily filled with particlesand the particles can detach during cleaning. Once the “dead pores” arefilled with particles, these “pores” are difficult to clean and the particles are trapped and cannot be removed. Dead pores can also be a result of the recapture of loosenedaerosols during the cleaning process. For example, during backpulse, an aerosol is detached from a nanofiber downstream of the filter. While migrating inside the filter toward the upstream end as carried by the airflow, the aerosol is intercepted by

nanofibers in the upstream end of the filter and gets permanently captured. When the filter undergoes cleaning again, the shear force acting on the aerosol cannot overcome the adhesion force between the aerosol and the attached nanofiber; this is considered trapped in the “dead pore”. If these dead pores are located near the “front” of the filter, this further adds to the skin effect and gives rise to $\Delta P_{r,1}$ - ΔP_f in *Figure 5.2*.

Referring to *Figure 5.4(a)*, in the first hour of aerosol loading, the filtration mechanism of the nano-aerosols was depth filtration where aerosols started filling up the pores of the filter, and therefore, the rise in pressure drop was relatively slow. Between the second and fourth hour, there was a transition fromdepth tosurface filtration where the rise in pressure started to slow down. After the open pores near the upstream layer started to reduce (skin effect) to several aerosol diameters due to deposition of trapped aerosols, bridging of aerosols across the pores took place and additional aerosols weredeposited onto these “bridges”. Incoming aerosols started depositing onto the surface of the filter forming a growing cake. At this point, the cake became the filter media and the filter is under surface filtration. Very minimal amount of aerosols passed through the cake into the nanofiber filter. Air could still flow through the cake and the loaded filter through the open pores in the cake and the open pores in the filter. Note that cake or surface filtration has a characteristic of a linear rise of pressure drop excursion with aerosols loading time.

After the first loading cycle, including deposition of aerosols in the filter, especially at the upstream end of the filter forming the skin effect, and the buildup of cake, the subsequent cleaning by backpulse/backblow could only remove the cake and the aerosols in the depth of the filter.The skin layer (i.e. with more aerosol deposited near the upstream end of the filter) was still present. During reloading, the pressure drop increased steeply as the aerosol-laden air stream flowed through the filter depositing more aerosols onto the existing trapped aerosols in the skin layer which further restricted the flow passage. Eventually the pore opening between the nanofibers near the filter surface again reduced to several aerosol diameters for which bridging could occur again as aerosols jammed the mouth of the pore. Cake started to formagain around the pore, on the fiber surface, and onthe existing cake heel layer (residual cake left behind from previous backpulse and/or backblow).

In general, the cake is more permeable with lower flow resistance despite the cake layer thickness increases with aerosol deposit when compared to much higher flow resistance in the skin layer through continuously decreasing pore diameter from aerosols deposit onto the “walls” of the pore. This modulation in rise of pressure drop from the initial steep rise is represented by a concave shapecurve of pressure drop versus time. Subsequently, the filtration is dominated by cake filtration in which the pressure drop increases linearly over time or with specific mass deposit.

$$\Delta P = \Delta P_f^* + \Delta P_c \qquad \text{Eq. (14)}$$

$$\Delta P = K_f^* \mu U + K_c \mu U \cdot W \qquad \text{Eq. (15)}$$

$$W = c U A \cdot t_l \qquad \text{Eq. (16)}$$

$W \propto t_l$ (Assumingsteady loading)

The phenomenon has illustrated the fact that in the first cycle, when the pores are filled, and the filter structure and properties are changed with the particles trapped, the specific resistance factor of the filter mediumK_f^*increases with the aerosol deposit. On the other hand, during cake filtration, the cake is assumed to capture 100% of the incoming aerosols, therefore no aerosols reach the filter and hence K_f^* does not increase further. Assuming the specific cake resistance, K_c,and the specific resistance factor of the filter medium, including the captured particles in filter,K_f^*,do not change, the pressure drop varies linearly with mass deposit, Eq. (15). During cleaning, assuming the cake is completely removed,ΔP_c =0, yet some aerosols being detached from the nanofibers might redeposit back upstream in the filter leading to higher ΔP_f^*. From repeated loading, it can be seen that the slopes of the loading curves in cake filtration are practically the same indicating that under constant loading conditions, the specific cake resistanceremains

the same independent of the number of loading cycles as well ascleaning performed in between these loading cycles.

The slope of the curve in *Figure 5.4(a)*is given by:

$$\frac{d\Delta P}{dt} = K_c \, \mu \, U \cdot (c \, U \, A) \qquad \text{Eq. (17)}$$

One should be able to determine $K_c$from the results in *Figure5.4(b)*, where the slope of the curve is:

$$\frac{d\Delta P}{dW} = K_c \, \mu \, U$$

$$\frac{d\Delta P}{dW} = 343.11 \ \frac{Pa \cdot g}{m^2} (\text{from the graph}) \qquad \text{Eq. (18)}$$

Given that the face velocity and dynamic viscosity of air at$20℃$ are:

$$U = 0.053 \frac{m}{s} \qquad \text{Eq. (19)}$$

$$\mu = 1.82 \times 10^{-5} \ Pa \cdot s \qquad \text{Eq. (20)}$$

Therefore, the K_c can be determined from the above equations which equals to$3.59 \times 10^8 \frac{m}{g}$.

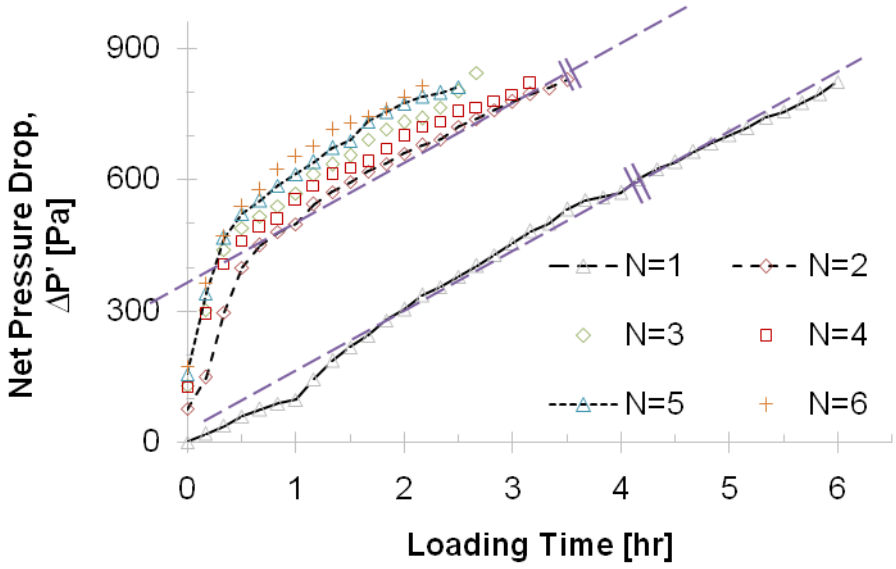
Net Pressure Drop, ΔP' [Pa]
900
600
300
0
0
1
2
3
4
5
6
Loading Time [hr]
N=1
N=2
N=3
N=4
N=5
N=6

(a)

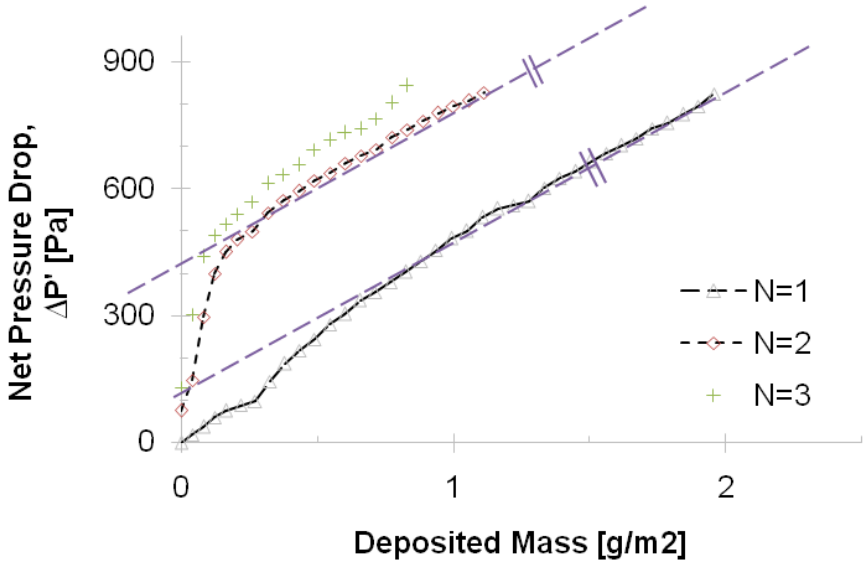
Net Pressure Drop, ΔP' [Pa]
900
600
300
0
0
1
2
Deposited Mass [g/m2]
N=1
N=2
N=3

(b)

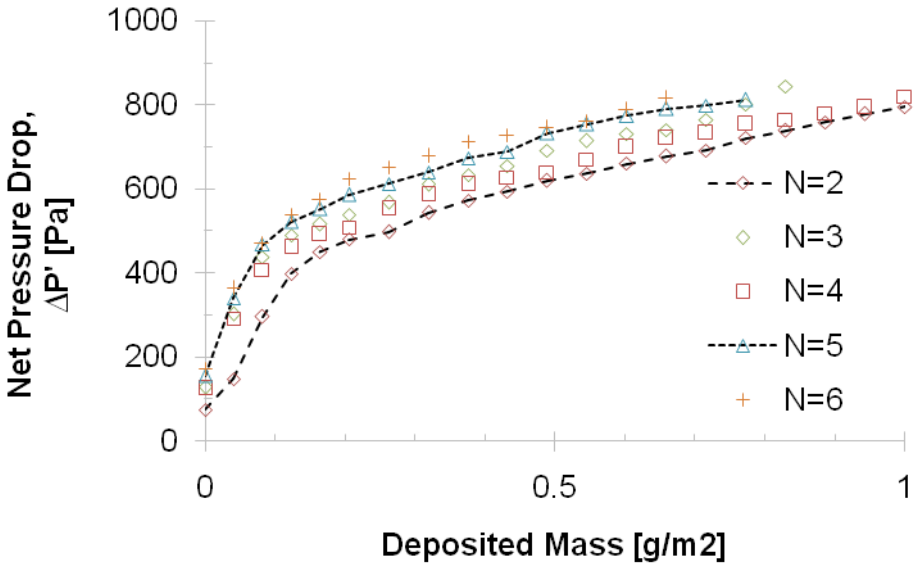

(c)

Figure 5.4Loading curve of the nanofiber filter (a) over time at different cycles, (b) over aerosol deposit at first three cycles, and (c) over aerosol deposit at cycles after first cycle

5.2. Multilayer Filter

The skin effect was confirmed to bepresentwhen loading a nanofiber filter and it inhibits the full utilization of the loading capacity of the nanofiber filter as more aerosols are deposited near the upstream end of the filter. This can be compensated by an inhomogeneous multilayer filter which enhances the aerosol loading distribution across the filter thickness (W.W.F. Leung, C.H. Hung, P.T. Yuen, 2009). In the experiments, microfiber-nanofiber filter arrangements were tested.The microfiber filter located upstream of the incoming flow has larger mean fiber diameterof 2μm,higher porosity, and larger filter thickness; while the nanofiber filter downstream has mean fiber diameter of only 180nm, lower porosity, and smaller layer thickness. In another arrangement, two nanofiber filters stacked together were tested. The upstream nanofiber filter has mean fiber diameter of 280nm while the downstream nanofiber filter has mean fiber diameter of 180nm. These tested inhomogeneous filters,abbreviated as MN (microfiber followed by nanofiber filter) and NN (nanofiber followed by nanofiber filter) arrangementsrespectively, are shown in *Figure 5.5(a) and Figure 5.5(b)*.

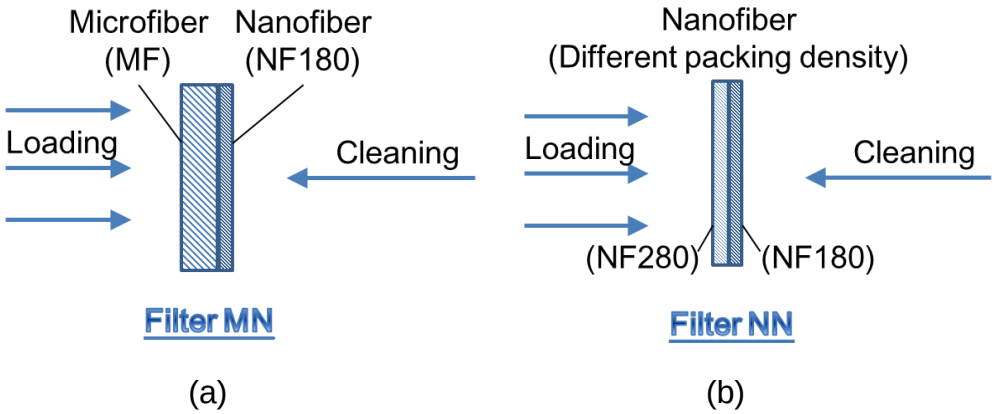

Figure 5.5Conceptual diagrams of multilayer filters: (a) Filter MN, (b) Filter NN

Filter MN was made up of an upstream microfibrous filter and immediate downstream a nanofiber filter. The overall pressure drop of clean Filter MN was 50Pa.

Filter NN was made by stacking two nanofiber layers and the overall pressure drop of the clean Filter NN before aerosol loading was 60Pa.

Compare the loading behaviour of Filter MN with Filter NN depicted in *Figure 5.6*,the former is relatively linear while the later had shown a concave downward shape in the beginning. Both loading had a transition state before become linear when reaching a relatively stable state. The two states had indicated the different loading mechanism occurred as mentioned in Section 5.1.

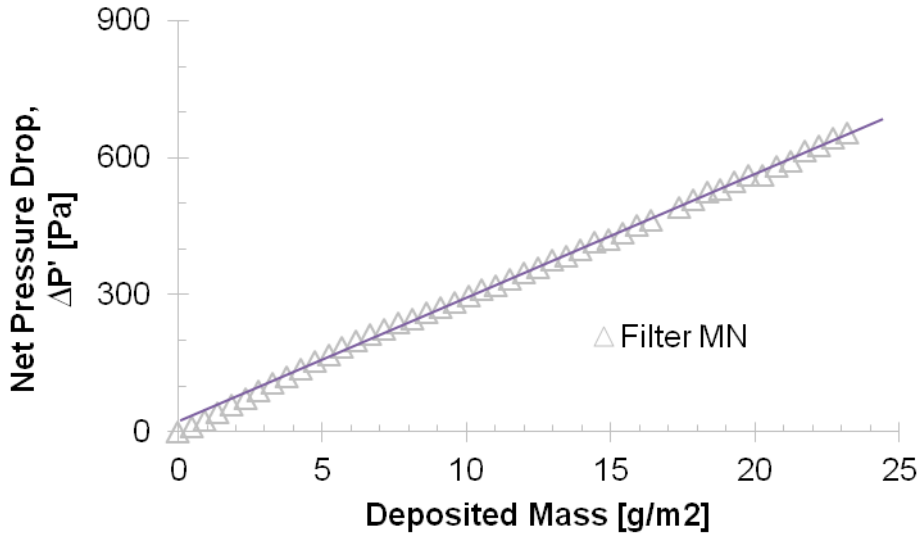

(a)

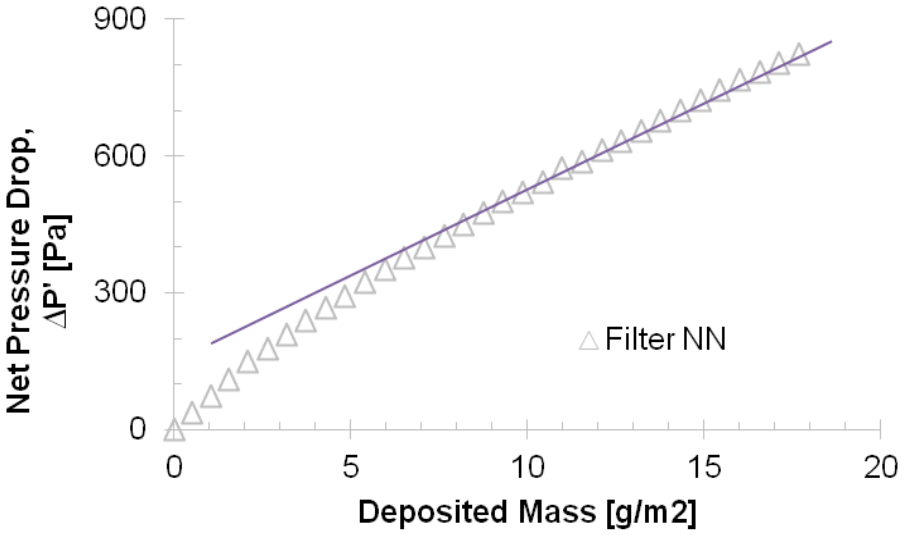

(b)

Figure 5.6 Loading curve over aerosol deposit of (a)Filter MN and (b) Filter NN

The filters were cleaned by combination of backpulse and backblow. The backpulse consisted of 0.5s pulse-jet, 0.2s idling with ten pulses as a unit. The backblow was 10s in between the series of backpulses. The

cleaning behaviour of multilayer filters was found to be similar to that of single layer nanofiber filter, with three stages, and thus, theregeneration of multilayer filter was also proved to be possible.

The results were compared with that of a single-layer filterin *Figure 5.7*. Two single-layer filters have undertaken the same loading and cleaning processes, one of them was a microfibrous filter, and the other one was ananofiber filter with mean fiber diameter of 280nm. These filters have the same filter properties corresponding to the upstream layer of Filter MN and Filter NN, respectively.

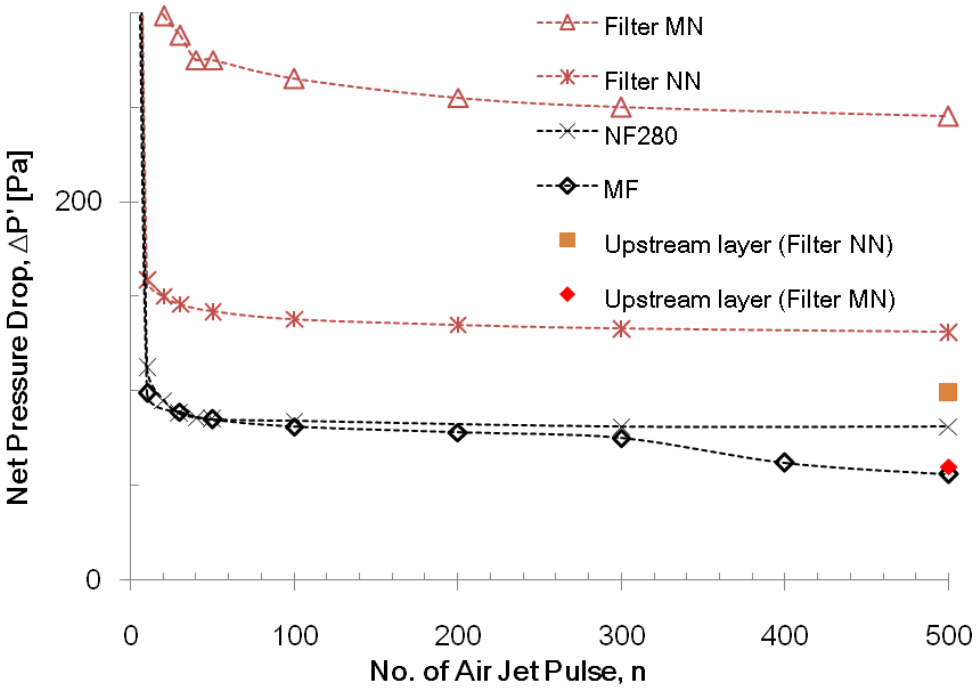

Figure 5.7The cleaning curves of multilayer filters when compared with single layer filters

Table 5.1 listed the residual pressure drop of the filters at 5.3cm/s. The overall residual pressure drop of the stacked filter was monitored throughout the test while the residual pressure drop of the separate layer was obtained only upon completion of the test. After the experiment stopped, the downstream layer was removed with minimal disturbance while the upstream filter layer remained mounted on the cleaning chamber. The pressure drop of the upstream filter layer was measured at the same face velocity of 5.3cm/s.The residual pressure drop of downstream layer was obtained from the difference between the measured overall residual pressure drop and the measured residual pressure drop of the upstream filter layer.

It isclearfrom *Table 5.1*that single-layer filter after cleaning can reach a lower residual pressure drop than that of a multilayer filter. As the number of layers stackedin a multilayer filter arrangement increases, the resistance of the filter would be higher to the airflow for cleaning. In other words, the airflow velocity for the same driving overpressure would be lower. The upstream layers of multilayer filters had a residual pressure drop higher than that of single layer with the same filter properties (81 vs. 77Pa for microfibrous filter). The difference of nanofiber filter waseven more significant (127 vs. 107 Pa). This is because the downstream layer (along the reversed flow direction during cleaning cycle) acts as a damper to the cleaning jet pulses and it becomes more difficult to remove aerosolstrapped inside the multilayer filter.

Multilayer Filter					
		Filter MN		Filter NN	
		Up	Down	Up	Down
Combination		MF	NF	NF	NF
Residual pressure drop, ΔP_r (Pa)	**Layer**	81	215*	127	67*
	Overall	296		194	

Single layer Filter		
	MF	NF280
Residual pressure drop, ΔP_r (Pa)	77	107

*Table 5.1Residual pressure drop of multilayer filters compared with single layer filters (*Note, these are back-calculated)*

During loading, Filter MN has shown a more uniform aerosoldeposition profile across the fiber mat thickness than Filter NN, as the upstream microfibrous filter has a larger aerosol holding capacity and reduce the formation of skin effect, thus the loading on the downstream nanofiber filter was more effective.

However, when the cleaning process began, the upstream microfiber caused a damping effect reducing the cleaning air jet momentum and enhancing the recaptureof loosen aerosol with consequence of ahigher residual pressure drop due to more deposit in the upstream skin layer of the nanofiber filter.

After making the comparison of the cleaning performances of inhomogeneous Filter MN, Filter NN and single layer, cyclic loading and cleaning were carried out on the multilayer filters.

Two multilayer filters, inhomogeneous Filter MN-2 and homogeneous Filter NN-2 were produced as depicted in *Figure 5.8*. FilterMN-2 was made up of microfibrous filter and nanofiber filter where the mean fiber diameters were 2μm and 120nm, respectively and the overall pressure drop of clean Filter MN-2 was 45Pa. Filter NN-2 was made by stacking two nanofiber layers where the mean fiber diameter was 120nmand the overall pressure drop of clean Filter MN-2 was 65Pa.

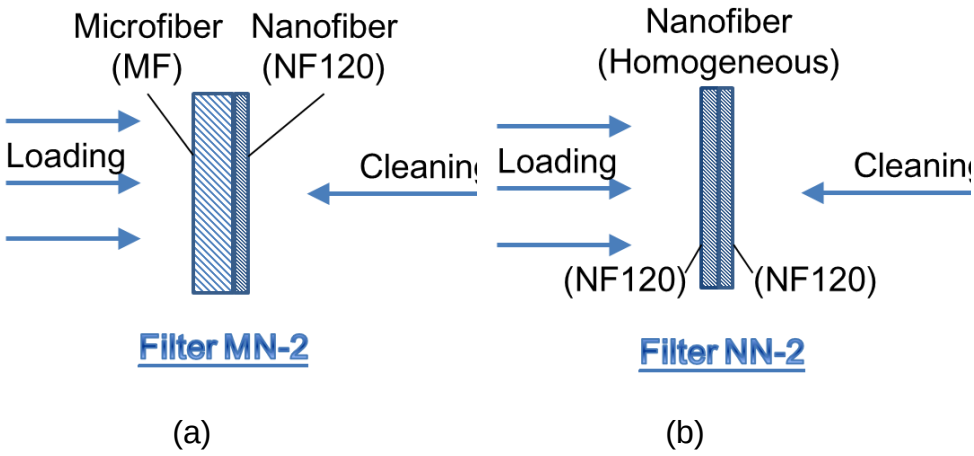

Figure 5.8Conceptual diagrams of multilayer filters: (a) Filter MN-2, (b) Filter NN-2

The cleaning conditions were different in the two cases and direct comparison cannot be made. The maximum allowable pressure drop was set at 1025Pa. The backpulse and backblow settings were the same in both cases, where the duration of pulse-jet, idling and backblow

were 0.5s, 0.2s and 10s respectively. The difference was the applied pressure.For Filter MN-2, the applied pressure was 5bar in the first three cleaning cycles and it was 6.5bar in the last two cycles. For Filter NN-2, the applied pressure was only 4bar at the beginning and afterward was increased to 5bar at the third cycle.

Figure 5.9 and *Figure 5.10* are the loading curves of Filter MN-2 and Filter NN-2 at different cycles. These multilayer filters had a similar cyclic loading behavior with single-layer filters (See *Figure 5.4*) that there was a distinct different at the first cycle with the later cycles. In addition, it is found from *Figure 5.9(b)* and *Figure 5.10(b)* that the loading for the later cycles had a similar behavior, it means that the filter media had a relatively constant filtration and loading properties.

However, looking at *Figure 5.9(a)* and *Figure 5.10(a)*, unlike single-layer cyclic loading, the slopes of the loading curves in cake filtration, i.e. the linear portion, were not the same in which the specific cake depends on the number of loading cyclesunder constant loading conditions.

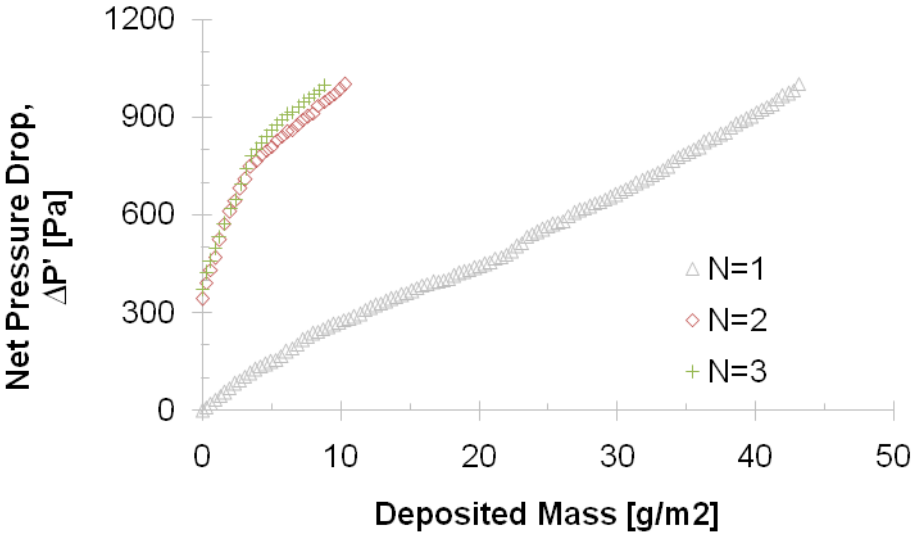

(a)

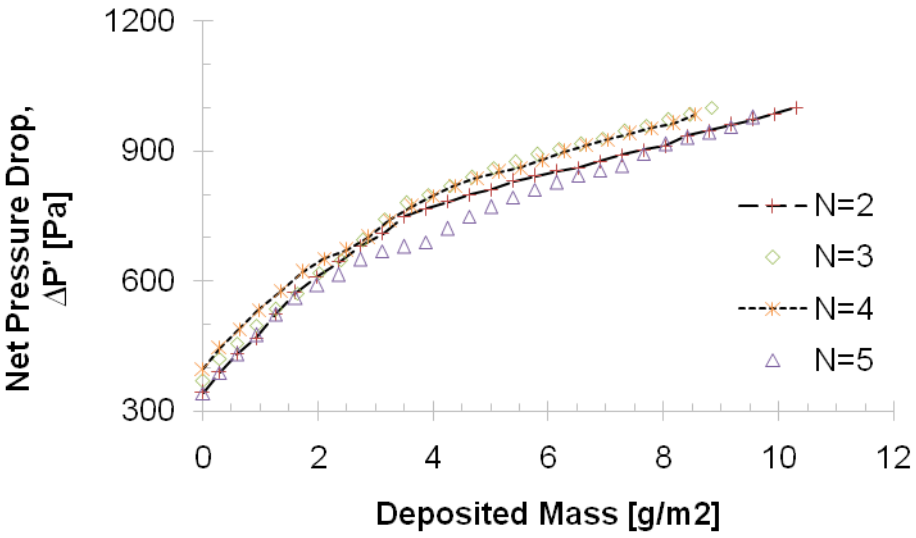

(b)

Figure 5.9Loading curve over aerosol deposit of Filter MN-2 (a) at first three cycles (b) at cycles after first cleaning

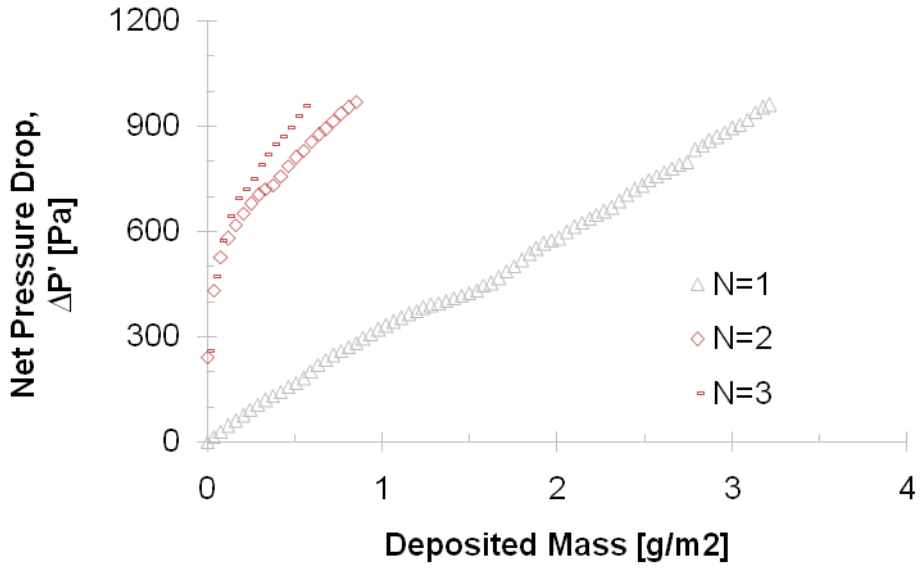

(a)

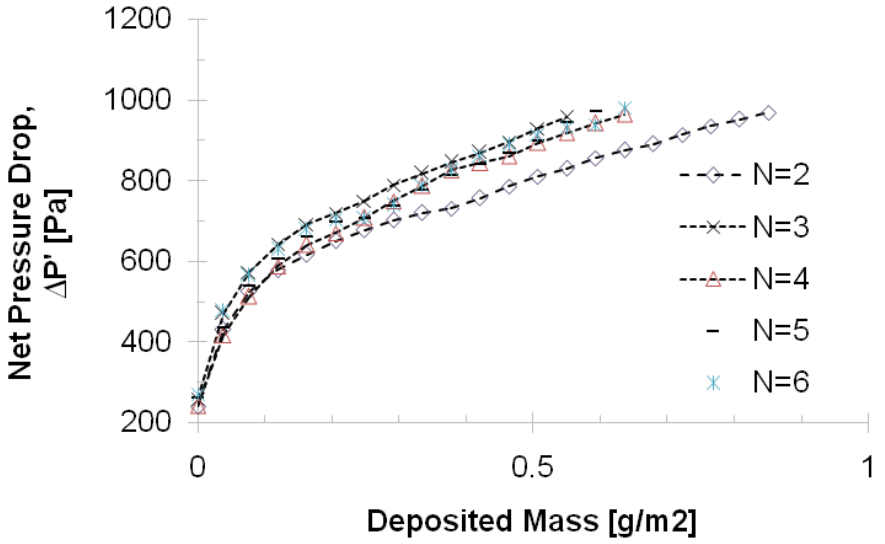

(b)

Figure 5.10Loading curve over aerosol deposit of Filter NN-2 (a) at first three cycles (b) at cycles after first cleaning

The overall cleaning behaviors were similar with a single layer filter undergoes cyclic loading in whichthe residual pressure drop built up gradually with filtration cycle, and filtration cycle time decreased dramatically after the first cycle, see *Figure 5.11*.Filter MN-2 and Filter

NN-2 have gone through five and six filtration cycles respectively where as indicated in the cleaning curve.Note that there was a change in applied pressure between the third and fourth cycle for Filter MN-2, and second and third cycle for Filter NN-2 as mentioned earlier. The increase in applied pressure enhanced the cleaning effectiveness, yetthe residual ratio did not show significant decrease.

The residual ratio and the cycle duration at each cycle were plotted in *Figure 5.12*. These samples have demonstrated a stable behavior (See *Section 5.1*). For Filter MN-2, the residual ratio from first to second cycle has risen from 0.34 to 0.37. The change was only 9% which is much lower compared to 70% with the single-layer case (*Figure 5.3),* whereas the percentage increase in the first two cycles of Filter NN-2 was 8% which was quite comparable. Due to the damping effect of the upstream layer during cleaning for a multilayer filter, the number of open pores, where the trapped particles at the position can be blown off during cleaning, is less than that in a single-layer filter. As a result, there is a structural change where the dead pores formed by the deposited particlesthat caused a tremendous change in single-layer case.

It has found that there was a sharp drop in cycle duration in the first cycle, after-which it was kept approximately constant in both cases. In the case of Filter MN-2, the loading and cleaning has taken close to 20 hours and subsequently it was kept constant in the range of 4 to 5 hours. While for Filter NN-2, the first filtration cycle took 13 hours to complete,

thereafter the duration was in the range of 3 to 4 hours. The results indicated a better stability with the multilayer filter for which the dead pores were more completely filled in the first cycle.

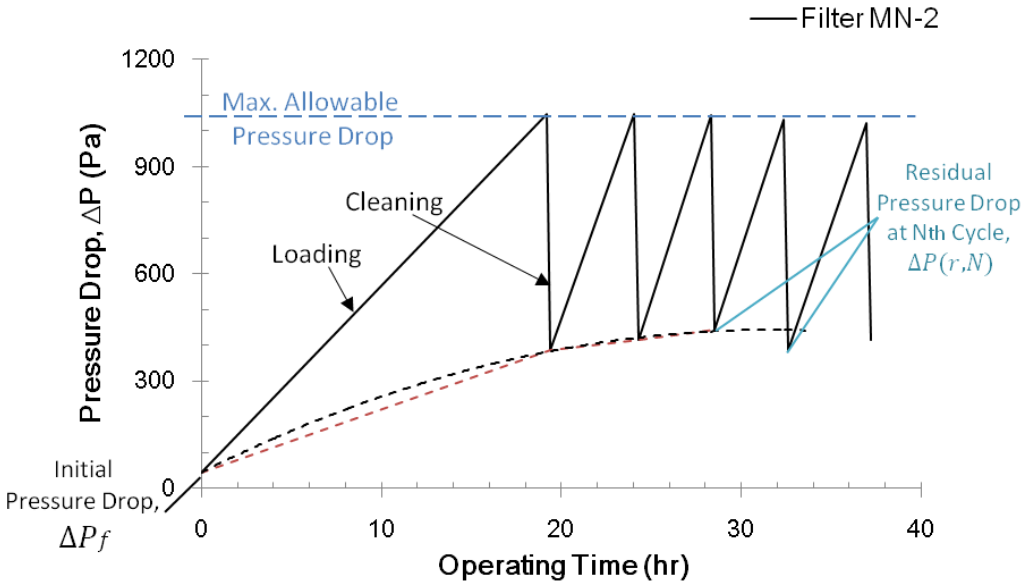

(a)

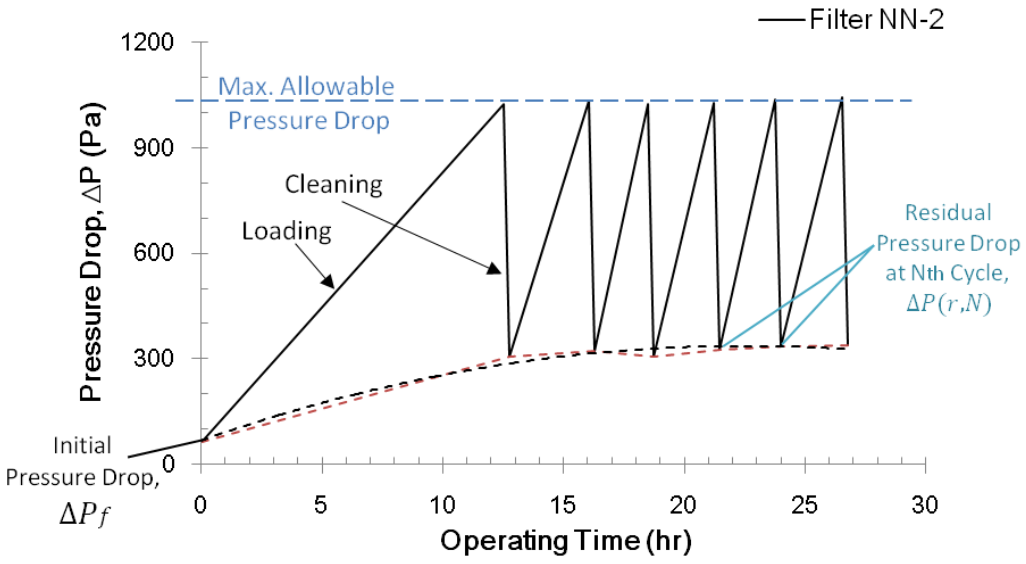

(b)

Figure 5.11Cleaning curve of cyclic loading on (a)Filter MN-2 (b)

Filter NN-2

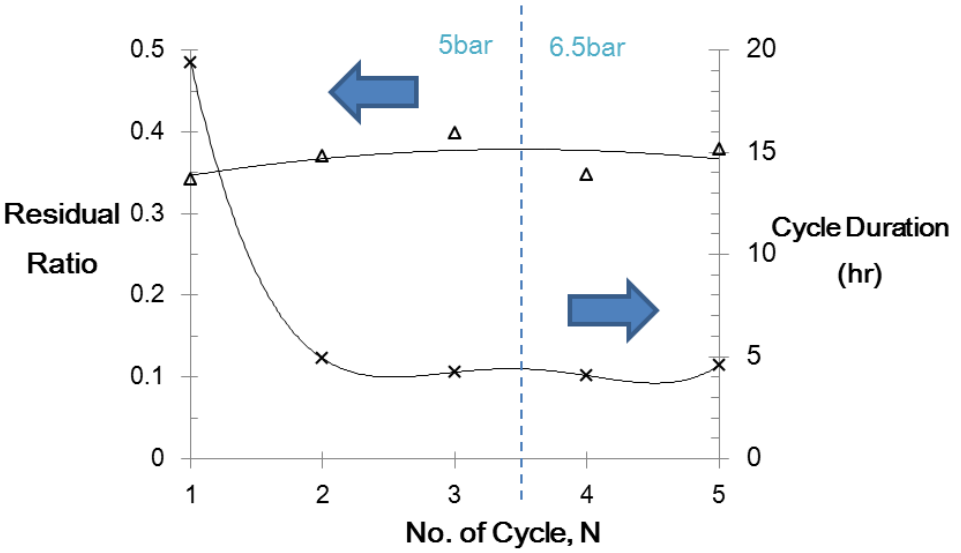

(a)

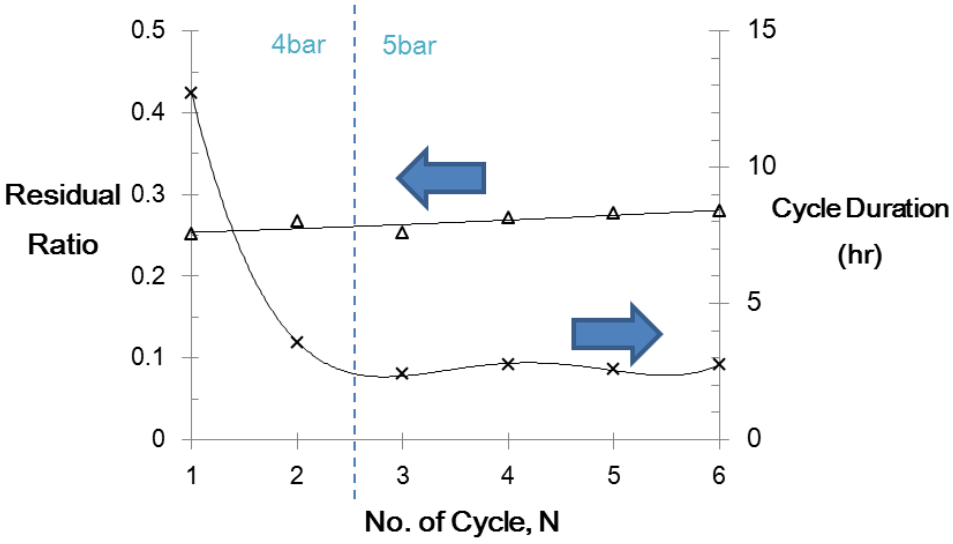

(b)

Figure 5.12the characteristic of residual ratio and the cycle duration of (a)Filter MN-2 (b) Filter NN-2

Chapter 6

CONCLUSIONS AND RECOMMENDATIONS FOR FUTURE RESEARCH

6.1. Conclusions

Nanofiber filter samples were fabricated successfully in a controlled operation by needle-less electrospinning with minimal beads and ribbon fibers. The filter properties, such as mean fiber diameter and fiber mat thickness (indirectly measured from pressure drop of the filter at 5.3cm/s) can change accordingly to the electrospinning conditions. For example, adjusting the effect of solution concentrations can significantly affect the fiber diameter, and the amount of fibers collected can be restricted by varyingthe travelling speed of the substrate during the electrospinning process.Other than the simpleconfiguration which has been investigated in details, threeother nanofiber filter configurations have also been developed to increase the “integrity” between electrospun nanofibers and the adjacent substrate to reduce tearing away of the nanofiber mat from the supportingsubstrate during backpulse and backblow cleaning.

Cleaning can be possible on a single-layer or multilayernanofiber filterusing backpulse and backblow as well as a combination of both. As seen from the results of the experiments, three cleaning stages can be observed with backpulse and backblow. With reference to the pressure drop across the filter, in the first stage there is a steep drop in pressure

reflecting loosening of the cake (made of aerosols) attached to the nanofiber filter. The second stage the pressure drop is modest reflecting loosely attached aerosols can be removed. Finally, in the third stage there is a slow decrease in pressure drop which reflects that it is much harder to remove the remaining aerosols that are firmly anchored to the nanofibers. This study has demonstrated that the tri-nozzle setup can minimize the single strong air jet pulse at the centerthat acts on a single spot breaking the nanofibers there yet leaving other areas of the filter unclean. Along that direction, the tri-nozzle arrangement provides a more uniform cleaning of the filter.

For a desired residual pressure drop, the time required for backblow cleaning can be six times of that of backpulse. Therefore, in terms of efficiency, backpulse is a better choice in filter regeneration. Moreover, without backblow the residual remaining is as much as 7% higher as loosened aerosol get reattached upstream in the filter, hence, in terms of effectiveness, backpulse followed by backblow is a better choice in filter regeneration.Results also reveal that the valve opening time is not major factor but increase the valve opening time can ensure that the impact pulse effectively acts on the fibers and deposited particle. Higher backpulse pressure up to 6.5 bars can effectively produce most backpulse and backblow, however, this is at higher risk of breaking of the nanofiber layer.

The cleaning effectiveness can be affected by the mean fiber diameter and fiber mat thickness. Less residual particles remain inside filter sample with larger mean fiber diameter for a thinner nanofiber layer. This is due to the weakeradhesion between submicron particles and larger fiber, as well as the smaller dust holding capacity with a thinner nanofiber layer.

Despite the skin effect can be minimized by stacking fiber mats with different packing density together to form multilayer filter, the cleaning performance is not as effective as with the single layer, due to the damping effect of downstream layer, and the recapture of loosen particles during cleaning. The cyclic filtrations in single-layer and multilayer nanofiber filter are quite stable. The loading behavior in first cycle is significantly different from the rest of the cycles because of the dead pores are being filled in the first cycle, which changes the configuration of the filter.

6.2. Recommendation for Future Research

In cleaning nanofiber filter, there are numerousparameters that can further improve the cleaning effectiveness, such as standoff distance from nozzle to the filter, nozzle diameter, nozzle head design, and the direction of the testing column (i.e. parallel or perpendicular to gravitational force). At present, a tri-nozzle design has been developed

as the best arrangement for the regeneration of nanofiber filter. More analysis can be done on the effect of venturi effect on deposited particles removal in a nanofiber filter during cleaning.In multilayer filter, the upstream layer practically acts as a cover of the downstream layer mitigating the cleaning effect by air jets. It may be possible to include the gravitational force (transverse to air flow) as a collection means for loosened aerosols to reduce the recapture phenomena.

Similar tothe existing cleanable microfibrous filter, to improve its cleaning effectiveness and make it more practical in application (i.e. online cleaning mode), the filter is designed as baghousefilter. The filter can be further pleated to increase the surface area for filtration as well as to facilitate cake removal from “cake cracking” during expansion of the bag.

In this investigation, the test material selected is Nylon 6, however, other materialssuch asPolyacrylonitrile (PAN)and Polyvinyl acetate(PVA), etc. can also be used to produce elecotrospun nanofibers for the filter.Some preliminary results on cleaning are shown in *Figure 6.1*for filter materials other than Nylon 6. Filters made from these materials are also cleanable despite the cleaning performance has not yet been optimised. Results from preliminary test as shown in *Figure 6.1*revealed the first stage with a steep decrease in pressure drop followed by a short second stage and subsequently the third stage, for which there is little drop in pressure with increasing jet pulses.

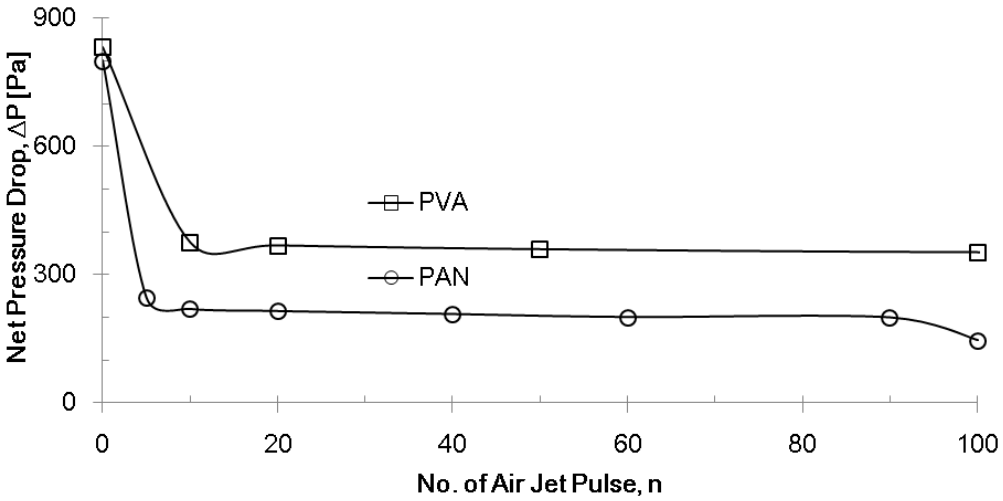

Figure 6.1 Cleaning curves of PVA and PAN nanofiber filters

References

M. De Ravin, W. Humphries, R. Postle. (1988). A model for the performance of a pulse jet filter. *Filtration and Separation, 25* (3), 201-207.

C. Huang, S. Chen, C. Lai, D. H. Reneker, H. Qiu, Y. Ye, H. Hou. (2006). Electrospun polymer nanofibres with small diameters. *Nanotechnology, 17*, 1558-1563.

D. Li and Y. Xia. (2004). Electrospinning of nanofibers: reinventing the wheel? *Advanced Materials, 16*, 1151-1170.

Dr.-Ing. P. Gäng. (2002). Update of VDI-Guideline 3926 "Testing of Filter Media for Cleanable Filters" and Development of a Mobile Filter Probe for Field Measurements. *6th Symposium "Textile Filters"* .

F . Rombaldoni, K. Mahmood, A. Varesano, M.B. Songia, A. Aluhi, C. Vineis, G. Mazzuchetti. (2013). Adhesion enhancement of electrospun nanofiber mats to polypropylene nonwoven fabric by low-temperature oxygen plasma treatment. *Surface & Coatings Technology, 216*, 178-184.

Formhals, A. (1934). *Patent No. US Patent 1975504.*

Formhals, A. (1939). *Patent No. US Patent 2160962.*

Formhals, A. (1940). *Patent No. US Patent 2187306.*

Formhals, A. (1943). *Patent No. US Patent 2323025.*

H.C. Lu, C.J. Tsai. (1998). A pilot-scale study of the design and operation parameters of a pulse-jet baghouse. *Aerosol science and technology, 29* (6), 510-524.

H.C. Lu, C.J. Tsai. (1999). Influence of design and operation parameters on bag-cleaning performance of pulse-jet baghouse. *Journal of Environmental Engineering, 125* (6), 583-591.

H.C. Lu, C.J. Tsai. (1996). Numerical and experimental study of cleaning process of a pulse-jet fabric filtration system. *Environmental science & technology, 30* (11), 3243-3249.

Hutten, I.M. (2007). *Handbook of nonwoven filter media.* Elsevier Ltd.

J. Doshi, D.H. Reneker. (1995). Electrospinning process and application of electrospun. *Journal of Electrostatics, 35*, 151-160.

J. Pich. (1966). Theory of aerosol filtration by fibrous and membrane filters. *London: C.N. Davies, Ed.: Aerosol Science, Academic Press* , 223-283.

J. Sievert, F. Löffler. (1989). Fabric cleaning in pulse-jet filters. *Chemical Engineering and Processing: Process Intensification, 26* (2), 179–183.

J.H. Choi, Y.G. Seo, J.W. Chung. (2001). Experimental study on the nozzle effect of the pulse cleaning for the ceramic filter candle. *Powder Technology, 114* (1-3), 129-135.

J.K.Lee, Y.Y.Ahn, S.K.Park, G.T.Kim, Y.H.Hwang, C.G.Lee, H.S.Shin. (2006). Development. *Current Applied Physics, 6*, 1030-1035.

James P. Lodge, Jr. (1988). *Methods of Air Sampling and Analysis.* CRC Press LLC.

L.M. Lo, D.R. Chen, D.Y.H. Pui. (2010). Experimental study of pleated fabric cartridges in a pulse-jet cleaned dust collector. *Powder Technology, 197* (3), 141-149.

M. Chowdhury, G. Stylios. (2010). Effect of experimental parameters on the morphology of electrospun Nylon 6 fibres. *International Journal of Basic & Applied Sciences, 10* (06).

O.G. Armağan, B.K. Kayaoğlu, H.C. Karakaş, F.S. Güner. (2013). Improving the adhesion strength of polypropylene nonwoven laminated fabrics using low-pressure plasma. *Fibres & Textiles in Eastern Europe, 21* (3), 99.

R. Mai, M. Fronhöfer, H. Leibold. (1996). Flow characteristics of filter candles during recleaning. *High Temperature Gas Cleaning* , 194-206.

R.C. Brown. (1993). *Air Filtration: An Integrated Approach to the Theory and Applications of Fibrous Filters.* Oxford: Pergamon Press.

S. LAUX, U. RENZ. (1993). Pressure cleaning of ceramic filter elements for the hot gas filtration. *Dissertation RWTH Aachen* .

S.K. Grannell, J.P.K. Seville. (1999). Effect of venture inserts on pulse cleaning of rigid ceramic filters. *High Temperature Gas Cleaning, 2*, 96-110.

W .W.F. Leung, C.H. Hung. (2012). Skin effect in nanofiber filtration of submicron aerosols. *Separation and Purification Technology, 92*, 174-180.

W .W.F. Leung, C.H. Hung, P.T. Yuen. (2010). Effect of face velocity, nanofiber packing density and thickness on filtration performance of filters with nanofibers coated on a substrate. *Separation and Purification Technology, 71*, 30-37.

W. Humphries, J.J. Madden. (1983). Fabric filtration for coal-fired boilers: dust dislodgement in pulse jet filters. *Filtration and Separation, 20* (1), 40-44.

W. Ren, C. Cheng, R. Wang, X. Li . (2010). Effect of fiber surface morphology on the hydrophilicity modification of cold plasma-treated polypropylene nonwoven fabrics. *Journal of applied polymer science, 116* (4), 2480-2486.

W.W.F. Leung, C.H. Hung, P.T. Yuen. (2009). Experimental investigation on continuous filtration of sub-micron aerosol by filter composed of dual-layers including a nanofiber layer. *Aerosol Science and Technology, 43* (12), 1174-1183.

Z.M. Huanga, Y.Z. Zhang, M. Kotakic, S. Ramakrishna. (2003). A review on polymer nanofibers by electrospinning and their applications in nanocomposites. *Composites Science and Technology, 63*, 2223-2253.